VOLUME 23 NUMBER 7 JULY 2021 www.env-micro.com ISSN 1462-2912

environmental microbiology

Special Issue on Ecophysiology of Extremophiles

Guest Editors: John E. Hallsworth Ricardo Amils, Kathleen C. Benison, Barbara Cavalazzi, Alfonso F. Davila, Michael T. Madigan, Laura Selbmann, Frances Westall

Mars' surface is not universally biocidal
Life in hot acid
Sub-lithic photosynthesis in hot desert habitats
Microbiology of a *salticle*
Solubilization and precipitation of rare earth elements by *A. niger*

WILEY

environmental microbiology

Environmental Microbiology (2021) **23**(7), 4034–4053 doi:10.1111/1462-2920.15617

Seasonal hydrologic and geologic forcing drive hot spring geochemistry and microbial biodiversity

Daniel R. Colman,[1] **Melody R. Lindsay**,[1] **Annette Harnish**,[1] **Evan M. Bilbrey**,[1] **Maximiliano J. Amenabar**,[1] **Matthew J. Selensky**,[1] **Kristopher M. Fecteau**,[2] **Randall V. Debes II**,[2] **Matthew B. Stott**,[3] **Everett L. Shock**[2,4] **and Eric S. Boyd**[1*]

[1]*Department of Microbiology and Immunology, Montana State University, Bozeman, MT, 59717.*

[2]*School of Molecular Sciences, Arizona State University, Tempe, AZ, 85287.*

[3]*School of Biological Sciences, University of Canterbury, Christchurch, 8140, New Zealand.*

[4]*School of Earth and Space Exploration, Arizona State University, Tempe, AZ, 85287.*

Summary

Hot springs integrate hydrologic and geologic processes that vary over short- and long-term time scales. However, the influence of temporal hydrologic and geologic change on hot spring biodiversity is unknown. Here, we coordinated near-weekly, cross-seasonal (~140 days) geochemical and microbial community analyses of three widely studied hot springs with local precipitation data in Yellowstone National Park. One spring ('HFS') exhibited statistically significant, coupled microbial and geochemical variation across seasons that was associated with recent precipitation patterns. Two other spring communities, 'CP' and 'DS', exhibited minimal to no variation across seasons. Variability in the seasonal response of springs is attributed to differences in the timing and extent of aquifer recharge with oxidized near-surface water from precipitation. This influx of oxidized water is associated with changes in community composition, and in particular, the abundances of aerobic sulfide-/sulfur-oxidizers that can acidify waters. During sampling, a new spring formed after a period of heavy precipitation and its successional dynamics were also influenced by surface water recharge. Collectively, these results indicate that changes in short-term hydrology associated with precipitation can impact hot spring geochemistry and microbial biodiversity. These results point to potential susceptibility of certain hot springs and their biodiversity to sustained, longer-term hydrologic changes.

Received 5 October, 2020; revised 10 May, 2021; accepted 29 May, 2021. *For correspondence. E-mail eboyd@montana.edu; Tel. (406) 994-7046; Fax (406) 994-4926.

Introduction

Terrestrial hydrothermal systems integrate surface atmospheric processes with subsurface hydrologic and geologic processes yielding hot springs with an incredible array of geochemical compositions (Fournier, 1989; Nordstrom *et al*., 2009; Shock *et al*., 2010; Lowenstern *et al*., 2012; Colman *et al*., 2017) that support immense microbial biodiversity (Barns *et al*., 1994; Hugenholtz *et al*., 1998; Colman *et al*., 2019). Hot springs can be dynamic, and their geochemical compositions can vary on time scales that range from seconds, days, seasons, or even longer periods (Heasler *et al*., 2009; Hurwitz and Lowenstern, 2014). Variation in the geochemical composition of hot springs over these timescales is related to fluctuations in one or more of a thermal feature's three main components: water, heat and the subsurface flow path(s) that deliver fluids to springs (Hutchinson, 1978). Consequently, changes in any one of these components due to changes in heat flux from the volcanic system, seismic activity, ground deformation, or short- or long-term precipitation patterns would be expected to result in substantial fluctuations in the geochemistry and the microbiology of hot springs. Indeed, numerous studies, particularly those conducted in Yellowstone National Park (YNP), have documented temporal changes in the geochemistry of hot springs (Allen and Day, 1935; White *et al*., 1988; Fournier *et al*., 2002; Shock *et al*., 2005; Nordstrom *et al*., 2009; Shock *et al*., 2010), with short- and long-term changes in hot spring chemistry sometimes linked to seismic activity (Marler and White, 1977; Payne *et al*., 2019).

Isotopic analyses of water (δ^2H, δ^3H, and δ^{18}O) in hot springs indicate that recharge of deep hydrothermal aquifers sourcing YNP hot springs, at least in the northwestern region of YNP, is primarily driven by meteoric

precipitation (Pearson and Truesdell, 1978; Kharaka *et al*., 2002; Gardner *et al*., 2011). This is largely in the form of winter snow melt from surrounding mountain ranges, with estimates of recharge of the deep hydrothermal aquifers by infiltrating meteoric fluid taking place over time scales that span hundreds of years (Pearson and Truesdell, 1978; Gardner *et al*., 2011). Other studies suggest that waters in the deep hydrothermal aquifer of YNP originate from the melting and retreat of glaciers that covered much of the region during the late Pleistocene, suggesting even longer time scales of recharge (e.g. >∼10 000 years ago) (Sturchio *et al*., 1987; Rye and Truesdell, 2007). Recharge of shallow aquifers that can mix with deep hydrothermal fluids in individual geyser basins is driven by localized snow-melt and/or precipitation that can lead to water table fluctuations (White *et al*., 1988; Fournier *et al*., 2002). Despite a relatively detailed understanding of how hot spring geochemistry can change over time, very little is known of how such changes influence or are influenced by temporal dynamics in hot spring microbial biodiversity.

The Norris Geyser Basin (NGB) within the northwestern region of YNP is one of the most dynamic geyser basins in YNP and hosts >400 thermal features with highly variable geochemical compositions (White *et al*., 1988). The groundwater at NGB is thought to comprise two distinct water types, including a shallow, cool water aquifer system formed from recent meteoric (e.g. snow melt, rainwater) recharge and a deep, high-temperature hydrothermal water system formed from older, more deeply sourced waters (White *et al*., 1988; Fournier *et al*., 2002; Gardner *et al*., 2011). Extensive changes in the geochemistry of hot springs have been documented in NGB at spatial scales that range from individual springs to groups of springs and at temporal scales ranging from days to decades or longer (White *et al*., 1988, Fournier *et al*., 2002). For example, predictable, nearly synchronous changes in the discharge and geochemical characteristics of several springs in the NGB have been documented in the late summer in what has been referred to as an annual disturbance (White *et al*., 1988, Fournier *et al*., 2002). The exact causes of this disturbance remain unknown but are thought to be related to fluctuations in the local water table due to seasonal recharge of aquifers sourcing these springs (White *et al*., 1988, Fournier *et al*., 2002).

Hot springs within the NGB host diverse microbial communities that are discretely distributed along spatial geochemical gradients (Langner *et al*., 2001; Donahoe-Christiansen *et al*., 2004; Macur *et al*., 2004; Spear *et al*., 2005; Boyd *et al*., 2007; Kozubal *et al*., 2012; Inskeep *et al*., 2013a; Inskeep *et al*., 2013b; Colman *et al*., 2016). At temperatures exceeding the upper limit of photosynthesis (∼73°C), members of these communities are supported by chemical energy in the form of disequilibria in electron donor and acceptor pairs that result from mixing of reduced deep hydrothermal fluids with more oxidized surface fluids (Shock *et al*., 2010; Colman *et al*., 2019). As such, seasonal differences in the relative input of deep reduced waters and near-surface oxidized waters would be expected to drive variation in the availability of electron donors and acceptors capable of supporting chemosynthetic microbial communities. Yet, only a few studies with limited (e.g. once per season) sampling scales have ever evaluated temporal hot spring community dynamics in YNP or elsewhere (Macur *et al*., 2004; Wang *et al*., 2014; Ward *et al*., 2017) and none have examined the link between geochemical and microbial community compositional changes as they relate to seasonal differences in the sources of fluids in hot springs. Consequently, little is known of the variation in hot spring community biodiversity over time scales that may be relevant for microbial population turnover and how it may be related to spring geochemical characteristics that vary with seasonal hydrologic changes.

Here, we coordinated near-weekly sampling of three widely studied hot springs in the NGB over a seasonal (∼140 day) period. A fourth hot spring in the vicinity of these three springs formed over this sampling interval and was included in the study to investigate successional geochemical and microbial dynamics and whether these were also associated with seasonal hydrologic changes. Data from aqueous geochemical and isotopic analyses were paired with local precipitation data to begin to constrain the source of fluids in each spring and the extent that they may be influenced by localized meteoric water recharge or other hydrologic changes. Concomitantly, deep sequencing of 16S rRNA genes was used to uncover feedbacks between seasonal variation in geochemical composition and microbial community composition. 16S rRNA gene data were used to identify metagenomic assembled genomes (MAGs) for use in predicting the functional potential of responsive populations and to predict the mechanisms underpinning their positive or negative responses to geochemical change. The results are discussed in terms of differences in the responsiveness of the aquifers sourcing hot springs to recharge with oxidized meteoric water, the extent that this influences the composition and functions of the microbial communities in these springs, and the potential longer-term consequences of altered aquifer recharge that may accompany changes in the hydrology of NGB.

Results and discussion

Sample site description

Three springs in YNP were sampled between 23 June, 2016 and 9 November, 2016 and are all located within

~500 m of each other in the One Hundred Springs Plain (OHSP) of the NGB (Supplementary Fig. S1). Briefly, 'HF' Spring (HFS) is a moderately sized (~3 m in diameter) pool that occasionally exhibits elemental S^0 deposition at its margins, does not have an outflow channel (Supplementary Fig. S1; Supplementary Fig. S2) and has been studied since at least 2009 (Hamilton *et al*., 2011). 'Dragon' Spring (DS) emanates from within a small shelf, forming a runoff channel that joins other spring channels that flow into Tantalus Creek. DS is characterized by the deposition of solid-phase S^0 near the spring source and along the primary spring runoff channel, with iron (hydr) oxides also deposited adjacent to the elemental S^0 and at lower temperature (Supplementary Fig. S1; Supplementary Fig. S3). This spring has been the subject of detailed geochemical and microbiological study since at least 1998 (Langner *et al*., 2001). Cinder Pool (CP) is a large (~9 m diameter) pool without an outlet that harbours a pool of molten S^0 at ~18 m depth (Allen and Day, 1935; White *et al*., 1988). The molten S^0 at depth gives rise to centimetre-sized black spherules that are comprised of S^0 (~99.5%) with dispersed FeS_2 (~0.5%) and that coalesce at the water surface (Supplementary Fig. S1; Supplementary Fig. S4). The earliest scientific accounts of CP are from 1927 (Allen and Day, 1935) and subsequent geochemical and microbiological investigations (White *et al*., 1988; Xu *et al*., 2000; Spear *et al*., 2005; Kamyshny Jr. *et al*., 2014; Urschel *et al*., 2015; Colman *et al*., 2016) suggest a relatively stable geochemical composition prior to this study. DS is present on the western end of the OHSP across a small surface hydrologic divide from CP and HFS (Supplementary Fig. S1).

The fourth spring of the study, hereafter referred to as 'New' Spring (NS), has to the authors' knowledge not been previously investigated in microbiological or geochemical studies of NGB. The only scientific description of this spring comes from the observations of Allen and Day, 1935 (Supplementary Fig. S5), wherein a spring located in approximately the same location as NS (Supplementary Fig. S5) is referred to as a 'perpetual spouter' (Allen and Day, 1935). NS has not been observed in previous yearly sampling of this area over a 25 year period by the authors, including even ephemeral activity. However, notes taken in 1984 by citizen scientists who monitor geysers in YNP describe an unnamed feature ~35 ft (~12 m) NNE of CP (consistent with the location of NS) that was also observed in Allen and Day (1935), with last known 'spouter' activity taking place in 1974–1975 (M.A. Bellingham, personal communication). During the sampling campaign described herein, NS began flowing from a fissure that had been covered with geyserite gravels at some time between sampling events on 16 September and 23 September (Supplementary Fig. S6). NS remained active until at least September 2019, but the spring had gone dormant based on several observations between April 2020 and May 2021. The minerals that precipitated as this spring developed were visually identified as S^0 and, later in the sampling period, iron (hydr)oxides, both of which appeared to accumulate over time (Supplementary File 1).

Daily precipitation records indicate that the early and later summer/autumn periods in NGB were characterized by increased precipitation compared to mid-summer (Fig. 1). These differences were used to empirically divide the sampling period into three seasonal precipitation regimes (Fig. 1). The early summer sampling period encompassed 25 days between 23 June (the first sampling day; Julian day, J.D., 175) and 18 July (J.D. 200) and was associated with a total of 73 mm of precipitation (Fig. 1). The late summer/autumn sampling period (5 September to 4 November; J.D. 249–309) comprised 61 days and was associated with 474 mm of precipitation. In contrast, the mid-summer period encompassed 48 days between 19 July and 4 September (J.D. 201–248), with a total of 34.5 mm of precipitation recorded.

Summary of fluid sources to NGB hot springs

Infiltration of the crust by meteoric water to depths of up to 5 km and interaction of this water with partially molten

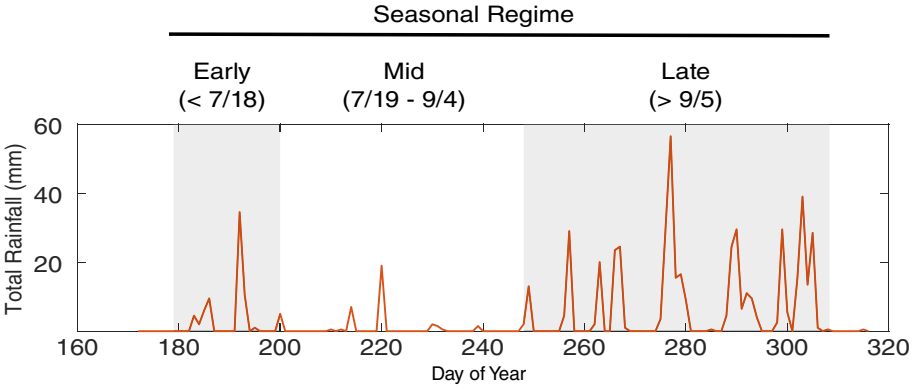

Fig. 1. Precipitation data in the local Norris Geyser Basin (NGB) area during the sampling period. Total daily rainfall observed in the NGB, as measured at the UNAVCO NGB borehole weather station. The sampling period between 23 June, 2016 (Julian day 175) and 9 November, 2016 (Julian day 314) was empirically separated into three periods corresponding to differences in early, mid, and late summer precipitation, as indicated by grey shading. [Color figure can be viewed at wileyonlinelibrary.com]

ductile rock results in subsurface water temperatures estimated to be >350°C that drive the YNP hydrothermal system (Craig *et al*., 1956; Fournier, 1989). The current model for the formation of hot springs in YNP begins with the injection of deep hydrothermal waters with volcanic gases including CO_2 and SO_2, the latter of which can disproportionate in aqueous fluids at high temperature to form SO_4^{2-} and H_2S (Nordstrom *et al*., 2009). These waters can ascend to the surface and undergo decompressional boiling leading to their separation as a circumneutral liquid phase enriched in solutes (e.g. chloride, Cl^-, and to a much lesser extent, SO_4^{2-} resulting from disproportionation) and a vapour phase enriched in gases including H_2S (Fournier, 1989; Nordstrom *et al*., 2005; Nordstrom *et al*., 2009). Condensation of gas-rich vapour with near-surface-oxidized meteoric waters is thought to result in their enrichment with H_2S that can then be oxidized, resulting in the production of sulfate (SO_4^{2-}) and protons/acidity (Nordstrom *et al*., 2005, Nordstrom *et al*., 2009). Importantly, H_2S oxidation at low pH (e.g. pH < 4) is kinetically inhibited (Zhang and Millero, 1993; Boyd, unpublished data), an observation consistent with the stability of H_2S in DS source waters in the absence of live cells (D'imperio *et al*., 2008). Furthermore, abiotic S^0 oxidation does not occur at temperatures <100°C (Nordstrom *et al*., 2005). Together, these data, at least partially implicate microbial H_2S/S^0 oxidation activities in the production of SO_4^{2-} and protons/acidity in hot springs, as has been suggested previously (Brock and Mosser, 1975; White *et al*., 1988; Colman *et al*., 2018) (*see* Supplementary Materials for additional discussion).

Based on the above framework, the source of fluids in hot springs can generally be identified by comparing the concentrations of Cl^- and SO_4^{2-} (White *et al*., 1988; Fournier, 1989; Nordstrom *et al*., 2009). Specifically, hydrothermal waters can be classified as meteoric waters with low concentrations of Cl^- and SO_4^{2-} (i.e. meteoric only waters; MO) and hydrothermal waters that have high concentrations of Cl^- (~330 mg L^{-1}) and moderate concentrations of SO_4^{2-} (70–100 mg L^{-1}; i.e. hydrothermal only; HO). Boiling and evaporation of waters can concentrate Cl^- and SO_4^{2-} (e.g. hydrothermal water + boiling; HB). Furthermore, input of H_2S-containing vapour into these two water types can result in increased SO_4^{2-} concentrations (e.g. meteoric water + gas (MG) or HB + gas (HBG)).

Application of this classification scheme to the springs sampled here suggests that DS and NS are sourced primarily by HO waters, while HFS hosts HO waters that have a greater MG component (Fig. 2A). The high Cl^- contents of all three spring waters, combined with their relatively high levels of sulfide and low pH (Supplementary Table S1), are consistent with previous interpretations of a shallow, Cl^-- and SO_4^{2-}-rich aquifer in the NGB that is infused with vapour phase gases enriched with sulfide and that is variably mixed with HO waters (White *et al*., 1988; Fournier *et al*., 2002). In contrast to waters from the other three springs, CP waters are more reflective of HO waters that have undergone boiling and evaporation, as indicated by high Cl^-

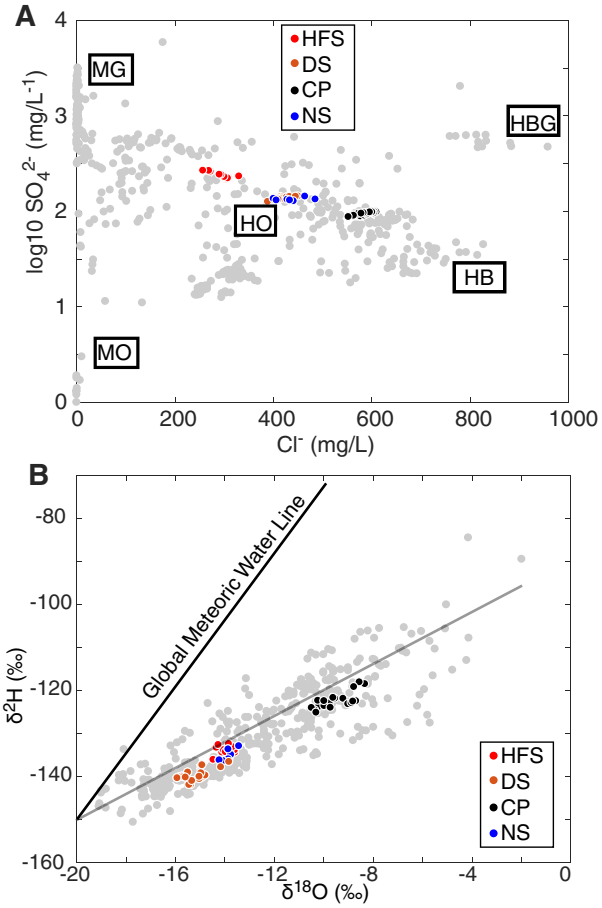

Fig. 2. Overall geochemical profiles for four Norris Geyser Basin (NGB) springs.
A. Sulfate (SO_4^{2-}) and chloride (Cl^-) concentrations. Data are shown for 'HF' Spring (HFS) in red, 'Dragon' Spring (DS) in dark orange, Cinder Pool (CP) in black, and 'New' Spring (NS) in blue circles, with additional data for 488 Yellowstone National Park (YNP) springs shown for comparison as grey circles. Previously described hot spring water type compositions (Nordstrom *et al*., 2009) are indicated as follows: MG, meteoric water infused with gas; MO, meteoric water only; HO, hydrothermal water only; HB, hydrothermal waters that have undergone boiling; and HBG, hydrothermal waters that have undergone boiling with hot gas recharge.
B. Water isotopes (δ^2H and $\delta^{18}O$) of hot spring waters for HFS, DS, CP, and NS, as coloured in panel (A). The global meteoric water line (GMWL; defined as $\delta^2H = 8 \times (\delta^{18}O) + 10$; following Craig (1961)) is plotted in black and the trend for typical evaporating hydrothermal waters in YNP is plotted in light grey with a slope of ~3, following Nordstrom *et al*. (2009). The plot is drawn with the intercept of the GMWL and the inferred evaporative trend for YNP waters at the δ^2H and $\delta^{18}O$ values for estimated recharge waters for the YNP hydrothermal system, as estimated in Kharaka *et al*. (2002). [Color figure can be viewed at wileyonlinelibrary.com]

concentrations (Fig. 2A) (Nordstrom *et al*., 2009). This observation may be consistent with the near-boiling surface temperature of CP and the absence of a surface outlet for spring waters.

To examine if precipitation potentially influences hot spring water compositions through dilution of the near-surface aquifers sourcing these springs, water isotope (δ^2H and δ^{18}O) values were examined. Variation in water isotope values can reflect whether the hydrothermal waters sourcing a spring are potentially diluted by recent meteoric water input, as noted by isotopic values that plot closer to those of the global meteoric water line (GMWL; Fig. 2B). The GMWL represents the average annual relationship between hydrogen and oxygen isotope (δ^{18}O and δ^2H) ratios in natural meteoric waters. Water isotopes can also be substantially influenced by water–rock interactions; the reader is referred to (Rye, 1993) for such discussions. Estimates suggest that the waters recharging the deep hydrothermal aquifer in YNP have δ^2H and δ^{18}O values of $-149‰$ and $-19.9‰$ respectively (Kharaka *et al*., 2002) that can trend to isotopically more heavy values due to evaporation of lighter isotopes (Truesdell *et al*., 1977; Nordstrom *et al*., 2009), as shown in Fig. 2B. The δ^2H and δ^{18}O values measured for the four NGB waters sampled herein plot along a continuum of boiling/evaporation, with CP waters exhibiting considerably heavier isotope values compared to the other three springs. This is consistent with SO_4^{2-}/Cl^- measurements indicating that CP waters have likely been subjected to comparatively more boiling and evaporation. In contrast, DS, HFS, and NS water isotopic values are far less depleted and plot closer to the values for a hypothesized source water recharge for the YNP hydrothermal system (Fig. 2B). Details of the seasonal geochemical trends for each spring are presented below.

Summary of the taxonomic composition and functional potential of communities

To begin to characterize seasonal trends in the composition of microbial communities of the four springs, we sequenced 16S rRNA genes from planktonic biomass. A total of ~6.9 million quality-filtered 16S rRNA gene sequence reads were generated for 54 water samples from the four springs, with a few samples from each spring not yielding amplifiable 16S rRNA genes (Fig. 3). The communities were dominated by one or a few phylotypes, consistent with previous analyses of these hot spring communities (Langner *et al*., 2001; Donahoe-Christiansen *et al*., 2004; Macur *et al*., 2004; Spear *et al*., 2005; Boyd *et al*., 2007; Boyd *et al*., 2009; Kozubal *et al*., 2012; Inskeep *et al*., 2013a; Inskeep *et al*., 2013b; Colman *et al*., 2016; Colman *et al*., 2018) and acidic hot springs elsewhere (Ward *et al*., 2017). Specifically, three OTUs corresponding to an uncultured Sulfolobales sp., a *Hydrogenobaculum* sp. and an *Acidilobus* sp. comprise ~88% of the total quality-filtered sequences, with only six other archaeal OTUs contributing to ≥1% of the total dataset (Supplementary Table S2). Nevertheless, other less dominant OTUs contribute to variation among individual samples. For example, 11 OTUs contribute to >5% of several individual communities at varying sampling times and comprise the aforementioned three taxa in addition to OTUs related to the archaeal genera *Metallosphaera*, *Sulfolobus*, *Vulcanisaeta*, *Acidianus* and two uncultured Thaumarchaeota phylotypes phylogenetically distant from characterized taxa (Supplementary Table S2). Thus, these communities were primarily archaeal-dominated and taxonomically simple, as expected for high-temperature acidic springs (Ward *et al*., 2017; Colman *et al*., 2018).

The uncultured Sulfolobales OTU was prevalent in HFS (Fig. 3A) and dominant in CP communities (Fig. 3C), along with the *Acidilobus* OTU (Fig. 3A and C). *Hydrogenobaculum*, the only abundant bacterial genus, was particularly prevalent among certain spring communities including those of DS (Fig. 3B) and NS (Fig. 3D). Overall, community compositions were distinct among springs (Fig. 3E), although significant variability as a function of season was only observed for HFS (PERMANOVA; $R^2 = 0.51$, $p < 0.01$) and CP communities (PERMANOVA; $R^2 = 0.29$, $p = 0.05$). In contrast, variation in DS communities was not associated with season (PERMANOVA; $R^2 = 0.21$, $p = 0.189$). Lastly, the NS communities reflected successional patterns, transitioning from archaeal-dominated to bacterial-dominated, followed by an abrupt transition to archaeal dominance across its nearly 6 weeks of sampling (Fig. 3D).

The 11 most abundant OTUs across the dataset correspond to taxa whose energy metabolisms are predicted to rely on dissimilatory sulfur metabolisms, based on high 16S rRNA gene identity (>98%) to previously characterized isolates or MAGs (Supplementary Table S2). To evaluate inferred changes in the predicted functional capacity of the microbial populations that could be associated with seasonal changes, a database was generated comprising functional annotations for genomes or MAGs that are closely related (>98%), or identical, at the 16S rRNA gene level to the 11 abundant taxa across the communities. Functional profiles for each community were constructed based on the presence of protein-coding gene complements within the reference genomes (with a particular focus on dissimilatory sulfur metabolism) and were weighted by the 16S rRNA gene relative abundance of the corresponding population. The genomes were also surveyed for the presence of biochemical pathways involved in denitrification or nitrification (Supplementary

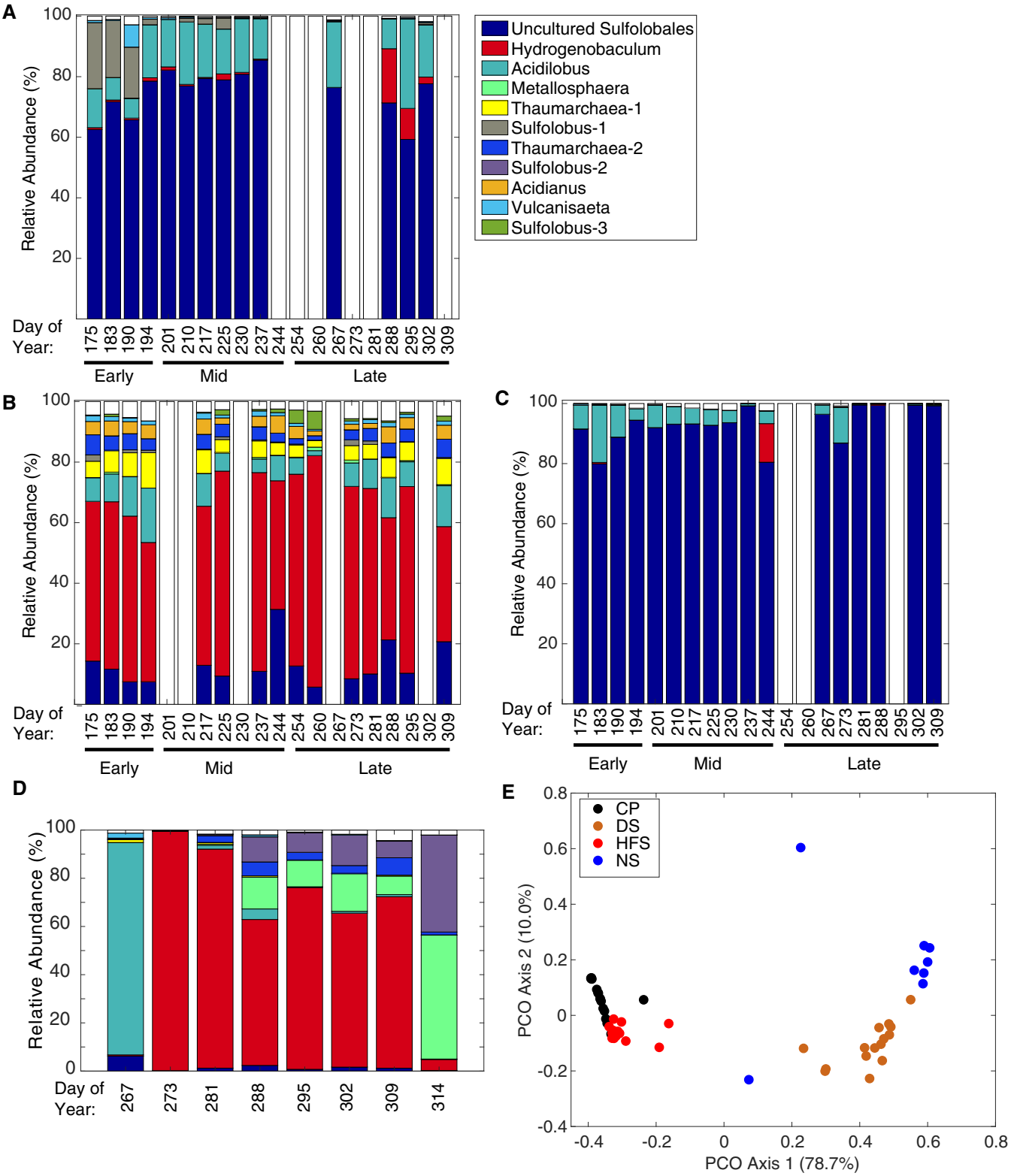

Fig. 3. Legend on next page.

Table S3), although only the *Vulcanisaeta* (overall relative abundance of ~2%) and *Metallosphaera* (~0.6%) genomes exhibited the potential capacity for denitrification (both via NarGHJI complements). Given the lack of inferred capacity for nitrogen-based metabolisms and the descriptions of closely related isolates (or MAGs) to the populations described here as being solely involved in sulfur-based metabolisms (Supplementary Table S2), we restrict the rest of the functional genomic discussion to pathways involved in sulfur biogeochemical cycling. Inferred community-wide, sulfur-based functional differences were highly significant among the four spring communities examined (PERMANOVA; $R^2 = 0.67$, $p \leq 0.001$), consistent with overall differences in their taxonomic compositions (Fig. 3E). In particular, the HFS and CP functional profiles were distinct from those of DS and NS (Fig. 4), with the potential exception of the NS samples from 23 September (J.D. 267) and 09 November (J.D. 314). These differences coincide with archaeal dominance in the HFS, CP, and the two aforementioned NS samples, in contrast to bacterial dominance in the DS and the remaining NS samples (Fig. 3).

Among these inferred functional differences, several components of Sulfolobales-based H_2S/S^0 oxidation pathways were inferred to be prevalent in HFS and CP communities, including terminal oxidase components (cytochrome $b_{558/566}$, Cbs; *Sulfolobus* oxidase, SoxLN, and *Desulfurolobus* oxidase, Dox), thiosulphate-quinone oxidoreductase subunits (Tqo) and heterodisulfide reductase subunits (Hdr) (Zeldes *et al*., 2019) (Fig. 4). In contrast, bacterial-based H_2S/S^0 oxidation pathways are predicted to be prevalent in DS and NS communities, including the sulfur-oxidizing protein (SoxYZBD) system, although many of the aforementioned Sulfolobales pathways are also predicted to also be moderately abundant in these samples. Furthermore, the capacity for S^0 reduction (e.g. via sulfur reductase, Sre; and a NAD(P)H sulfur oxidoreductase [Nsr]/ferredoxin:$NAD(P)^+$ oxidoreductase [FNOR] systems) was predicted to be more prevalent in the HFS and CP communities relative to the DS and NS communities. Lastly, the capacity to reduce SO_4^{2-}/HSO_3^- (via dissimilatory sulfite reductase, DsrAB; adenylylsulfate reductase, Apr; and sulfate adenylyltransferase, Sat) was predicted to be moderately abundant only in the DS and NS communities. These inferences were broadly consistent with the dominant taxa within each spring and their characterized (or inferred) metabolisms (Supplementary Table S2). Like analyses of the taxonomic composition of communities, inferred functional differences also exhibit broad seasonal differences, although to varying extents. Specifically, HFS exhibited significant differences in inferred functional profiles across seasons ($R^2 = 0.53$, $p < 0.01$), DS communities exhibited weakly significant differences in inferred functional profiles across seasons ($R^2 = 0.38$, $p = 0.04$), and CP exhibited functional differences that were not associated with season ($R^2 = 0.09$; $p = 0.76$). A more detailed discussion of the temporal variation in hot spring geochemistry, the aquifers sourcing them and their associated microbial communities over the sampling time frame follows for each of the four springs individually.

Seasonal variation in HFS geochemical and microbial community composition

The δ^2H and $\delta^{18}O$ values for HFS waters generally exhibited trends towards heavier values from early to mid-summer. Subsequently, the δ^2H values of HFS waters trended towards the GMWL in the later season samples, while $\delta^{18}O$ returned to values similar to those of the early season samples and also towards the GMWL (Fig. 5A). These observations point to increasing evaporation during the mid-summer (or decreased input from a more meteoric-influenced aquifer) followed by a shift back towards sourcing of waters that have been more diluted with meteoric waters towards late summer/autumn.

Consistently, HFS waters exhibited the highest conductivity and pH in the early to mid-summer, followed by decreases in the late summer/autumn (Fig. 5B). Most dramatically, SO_4^{2-} and Cl^- concentrations both remained relatively unchanged throughout the early and mid-seasons, followed by a notable increase in SO_4^{2-} concentration and a decrease in Cl^- concentration in late summer/autumn (Fig. 5B; Supplementary Fig. S7). These observations are consistent with increased meteoric water input into the local near-surface aquifer sourcing HFS during the late summer/early autumn that coincides with decreasing conductivity and decreasing Cl^- concentrations (Fig. 5B). At the same time, increased recharge

Fig. 3. Microbial community composition for hot springs sampled in this study. The relative abundances of 11 OTUs that contributed >5% relative abundance in at least one community from any individual sample are shown for (A) 'HF' Spring, (B) 'Dragon' Spring, (C) Cinder Pool, and 'New' Spring (D). The Julian date of the sample is shown at the bottom of each panel, along with the periods corresponding to early-, mid-, and late-season samples for each spring. NS only appeared during the late-season period and thus only eight samples are shown for it. The taxonomy of each OTU to the lowest identified taxonomic rank is indicated in the legend at the upper right, with abundances following the ordering from bottom to top. Samples that did not yield amplifiable 16S rRNA genes are indicated by white bars. A principal coordinates analysis (PCoA) of the samples from the four springs is shown in (E), with samples coloured according to the legend in the upper left. The percent of variation explained by the first two axes (as a function of relative eigenvector contributions) is shown on each axis. [Color figure can be viewed at wileyonlinelibrary.com]

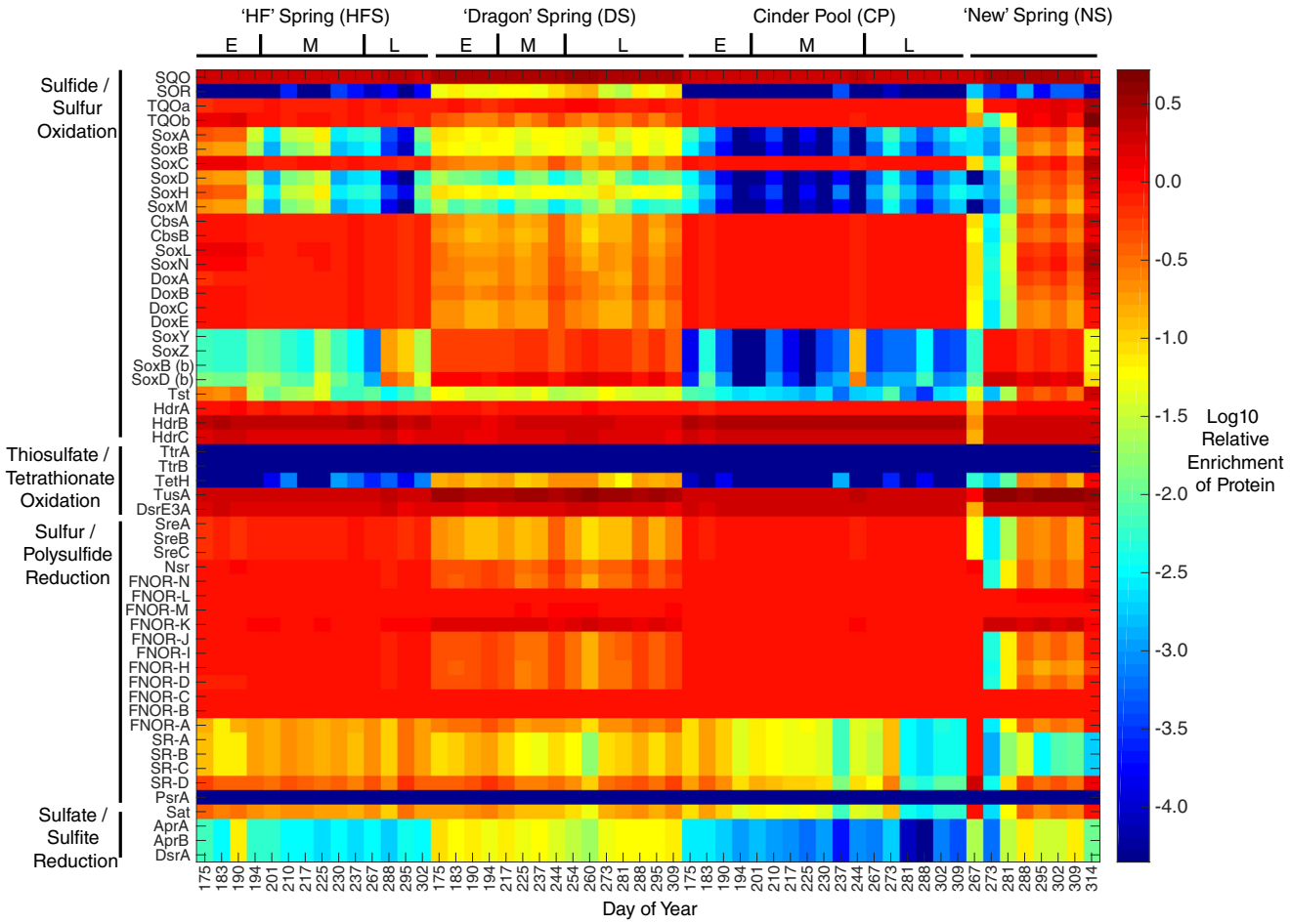

Fig. 4. Predicted dissimilatory sulfur metabolism functional potential of NGB communities. The heatmap shows the inferred relative enrichment of each protein homologue (on *Y*-axis) within each sample (on *X*-axis), based on the scale to the right (and as defined in the methods section). Protein homologues are grouped according to their broader classification within pathways. Abbreviations are described in Supplementary Table S3 along with reference information. The early ('E'), mid ('M') and late ('L') seasonal periods are indicated for each spring at the top of the heatmap. [Color figure can be viewed at wileyonlinelibrary.com]

with oxidized meteoric water may promote the oxidation of sulfide or S^0, potentially explaining the decrease in pH and increase in SO_4^{2-} concentrations (Nordstrom *et al*., 2005).

HFS waters were dominated by the uncultured Sulfolobales OTU, with the highest relative abundances in the mid-summer and lower relative abundances in the early and late summer/autumn periods (Fig. 3A). The representative 16S rRNA gene of the uncultured Sulfolobales OTU is nearly identical (99% nt identity; Supplementary Table S2) to those of MAGs previously recovered from YNP springs (Podar *et al*., 2013; Inskeep *et al*., 2013a; Inskeep *et al*., 2013b). A formal physiological characterization of these uncultivated organisms is lacking, but genomic inference suggests that they are likely supported by aerobic S^0 and/or H_2S oxidation (Podar *et al*., 2013; Inskeep *et al*., 2013a; Inskeep *et al*., 2013b), as is typical of most other Sulfolobales (Huber and Prangishvaili, 2006). The relative abundances of 16S rRNA gene sequences related to characterized aerobic S^0-oxidizing *Sulfolobus* spp. (Supplementary Table S2) were also prevalent in early season samples but nearly absent in the later season (Fig. 3A). In contrast, the relative abundances of 16S rRNA gene sequences affiliated with aerobic H_2- and H_2S/S^0-oxidizing *Hydrogenobaculum* sp. isolates were nearly absent in early and mid-summer but increased in the late summer/autumn (Fig. 3A; Supplementary Table S2). This variable abundance points to changes in ecological niches within HFS that are occupied by H_2S/S^0-oxidizing taxa over the seasonal sampling period. This is consistent with turnover in putative H_2S/S^0-oxidizing functional gene complements across seasons (Fig. 4) and with turnover in the

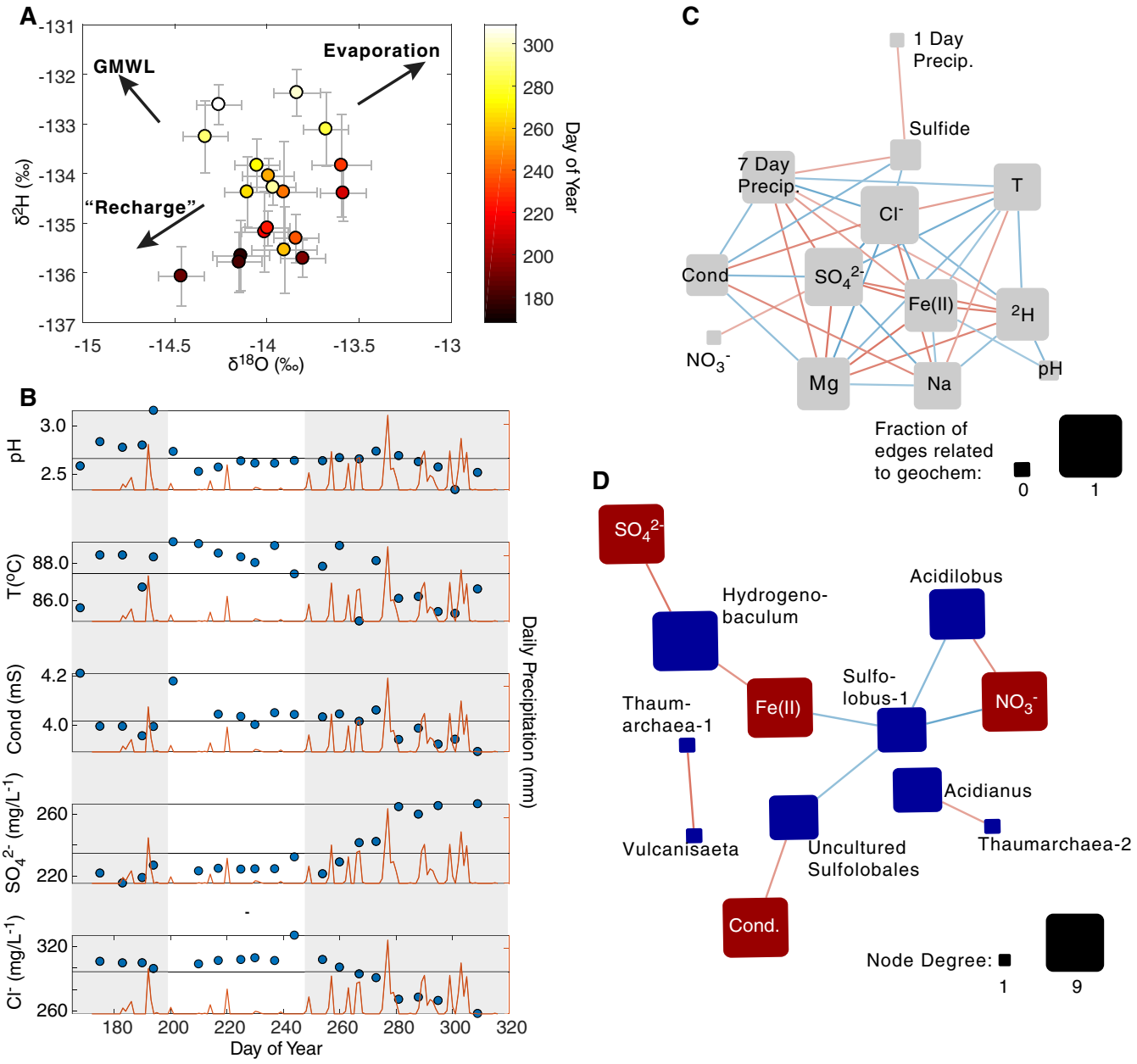

Fig. 5. Seasonal variation in 'HF' Spring (HFS) geochemical parameters and network analysis of associations among measured geochemical parameters and 16S rRNA gene operational taxonomic units (OTUs).

A. Water isotope values with each sample coloured according to the time scale next to the panel. Arrows are shown to indicate the general directions associated with water sources or processes (e.g. 'Recharge' representing the hypothesized recharge values for the YNP hydrothermal system discussed in Fig. 2A; GMWL indicating the relative position of the Global Mean Water line; and Evaporation indicated the inferred direction of change upon hydrothermal boiling/evaporation.

B. Seasonal trends for geochemical parameters. The Julian calendar days corresponding to when measurements were made or when samples were collected and preserved for measurement are shown. Geochemical data are overlaid on daily rainfall shown in the orange traces. The early and late seasonal periods are shaded in grey boxes to help delineate seasonal periods, as defined in Fig. 1. The average value for a specified measurement for each is indicated by a black line.

C. Network depicting significant correlations ($p < 0.05$) among geochemical parameters for HFS samples. Node sizing reflects fraction of edges related to geochemical parameters and is indicated by the scale to the bottom right of the network, with red edges indicating significant positive correlations and blue edges indicating significant negative correlations. Thus, larger-sized nodes represent geochemical parameters that exhibit more significant correlations to other geochemical parameters. Geochemical parameters without significant correlations to other parameters are not shown.

D. Network analyses of OTUs based on significant ($p < 0.05$) associations of their abundances with those of other OTUs and/or geochemical parameters. Node sizes are scaled to overall degree in the full network, as indicated in the bottom right of the figure, with edge colouring the same as in **(**C). Note that only geochemical parameters directly relevant to microbial metabolism are shown in this sub-network. The geochemical parameter nodes are all scaled to the same size, since the focus of the panel is to show the connectedness of OTUs to other OTUs and/or geochemical parameters only. Geochemical parameters that do not exhibit correlations to OTU abundances are not shown in these sub-networks. Geochemical parameter nodes are shown in red and OTU nodes are shown in blue. [Color figure can be viewed at wileyonlinelibrary.com]

taxonomic composition being significantly associated with season ($p \leq 0.001$; described above).

The prevalence of different putatively aerobic S-oxidizing taxa, albeit one a bacterium and the other an archaeon, in the early and late summer/autumn waters of HFS could be associated with differences in the availability of O_2 within spring waters across seasons. Increased oxygen availability could occur due to increased meteoric water input, which is generally more oxygen-rich, and that is inferred to contribute to HFS geochemical variation. Interestingly, although the inferred gene complements involved in H_2S/S^0 oxidation changed across seasons in HFS communities, these largely involved inferred changes in terminal oxidase proteins used by various Archaea (e.g. SoxABCM, CbsAB, SoxLN, and DoxABCE) and Bacteria (SoxYZ, SoxB, and SoxD) (Fig. 4). Differences in terminal oxidase complements among Sulfolobales have been suggested to be involved in adaptations to variable oxygen tensions, as demonstrated by cultivar growth experiments (Simon *et al*., 2009; Zeldes *et al*., 2019). Consequently, the turnover of populations harbouring different terminal oxidase complements may reflect taxonomic-level adaptations to varying oxygen availability within springs and warrants further investigation. Nevertheless, these changes likely contribute to variation in spring acidification via biotic aerobic H_2S and S^0 oxidation (Colman *et al*., 2018).

Correlational network analyses indicate that variation in the geochemical composition of HFS waters was largely associated with recent precipitation over a 7-day window (Fig. 5C), coinciding with the variation in HFS geochemical composition observed during the sampling period, and particularly later in the season after sustained heavy precipitation (Fig. 5B). Consistently, the correlational network analysis of OTU abundances in HFS communities indicates widespread associations of individual OTU abundances with variation in geochemical parameters (Fig. 5D). In contrast, direct network associations among OTUs of HFS are minimal (Supplementary Fig. S9), relative to the other springs examined (discussed below). These results collectively suggest that the aquifers sourcing HFS were responsive to meteoric recharge, and subsequent geochemical variation resulted in turnover of populations (e.g. *Sulfolobus* and *Hydrogenobaculum*) within HFS during the sampling period.

Seasonal variation in DS geochemical and microbial community composition

The DS isotopic values trended heavier during the mid-summer, while both the late summer/autumn δ^2H and $\delta^{18}O$ values for DS returned to similar values as observed in the early season samples. These observations may point to increased evaporation of waters sourcing DS in the summer (or less dilution from more meteoric recharge) followed by increased input of waters that have been diluted with meteoric water during the late-summer and early autumn. Relatively minor variation was observed for most geochemical parameters in DS waters (Fig. 6B), indicating that it may be primarily sourced by the deeper acid-sulfate-chloride reservoir theorized to be present in the subsurface of NGB (Truesdell *et al*., 1977; White *et al*., 1988; Fournier *et al*., 2002) and is less sensitive to local precipitation on the time scales measured herein.

In contrast to HFS, DS waters were largely dominated by a single *Hydrogenobaculum* sp. OTU, as previously reported for DS (Jackson *et al*., 2001; Boyd *et al*., 2009; Romano *et al*., 2013), with lesser contributions from uncultured Sulfolobales, *Acidilobus* sp., Thaumarchaeota phylotypes, *Sulfolobus* spp. and other Crenarchaeota (Fig. 3B). Although some seasonal variation in the abundances of these taxa were observed (Fig. 3B), and analysis of inferred functional variation across DS samples suggested a weak correlation to sampling period (discussed above), the relative abundances of populations generally did not differ markedly with seasons. Accordingly, DS community compositional variation was not associated with seasonal periods (PERMANOVA; $R^2 = 0.21$, $p = 0.19$). Unlike the correlational network analysis for HFS, that of DS indicates relatively little overall connectedness of geochemical variables (Fig. 6C), with recent precipitation only being correlated to a few parameters including SO_4^{2-} and Cl^- (which themselves were positively correlated; Fig. 6C). Thus, consistent with the above interpretations, the geochemical and microbial community composition of DS waters was minimally, if at all, responsive to recent precipitation.

Correlational network analyses of the variation in relative abundances of OTUs in DS indicate very few connections with variation in geochemical parameters, with the exception of the abundance of the 'Thaumarchaeota-2' OTU that was inversely correlated with temperature and positively correlated with SO_4^{2-} concentrations (Fig. 6D). A representative sequence from the OTU exhibits 99% nt identity with that attributed to a previously characterized Thaumarchaeota MAG in the Evening Primrose spring of YNP (Supplementary Table S2). The Evening Primrose thaumarchaeote was inferred to conduct heterotrophic SO_4^{2-} reduction in lower temperature, acidic hot springs, based on its inferred metabolic capacity and distribution across YNP springs (Payne *et al*., 2019). Thus, the predicted metabolic activity of this organism in DS, and its positive relationship to SO_4^{2-} and inverse relationship to temperature (Fig. 6D), potentially implicate this organism in SO_4^{2-} reduction in DS when the spring was cooler in temperature.

While correlational analysis indicates that population abundances did not strongly vary with geochemical differences, they were more strongly associated with abundances of other populations, as exhibited by low OTU connectivity to geochemical parameters and much higher among-OTU connectivity (Supplementary Fig. S9). Consequently, the turnover of communities in springs like DS may primarily be dictated by interactions among populations in the absence of strong, acute hydrologic forcing. If true, these interactions are likely occurring in the subsurface of DS since the source waters of this spring emit too rapidly (i.e. 0.2–0.5 m s^{-1}; estimated in (Takacs-Vesbach *et al.*, 2013)) to allow these interactions to play out in the spring source waters that were sampled.

Seasonal variation in CP geochemical and microbial community composition

CP isotope values exhibited more nuanced trends relative to the other spring waters, wherein shifts towards

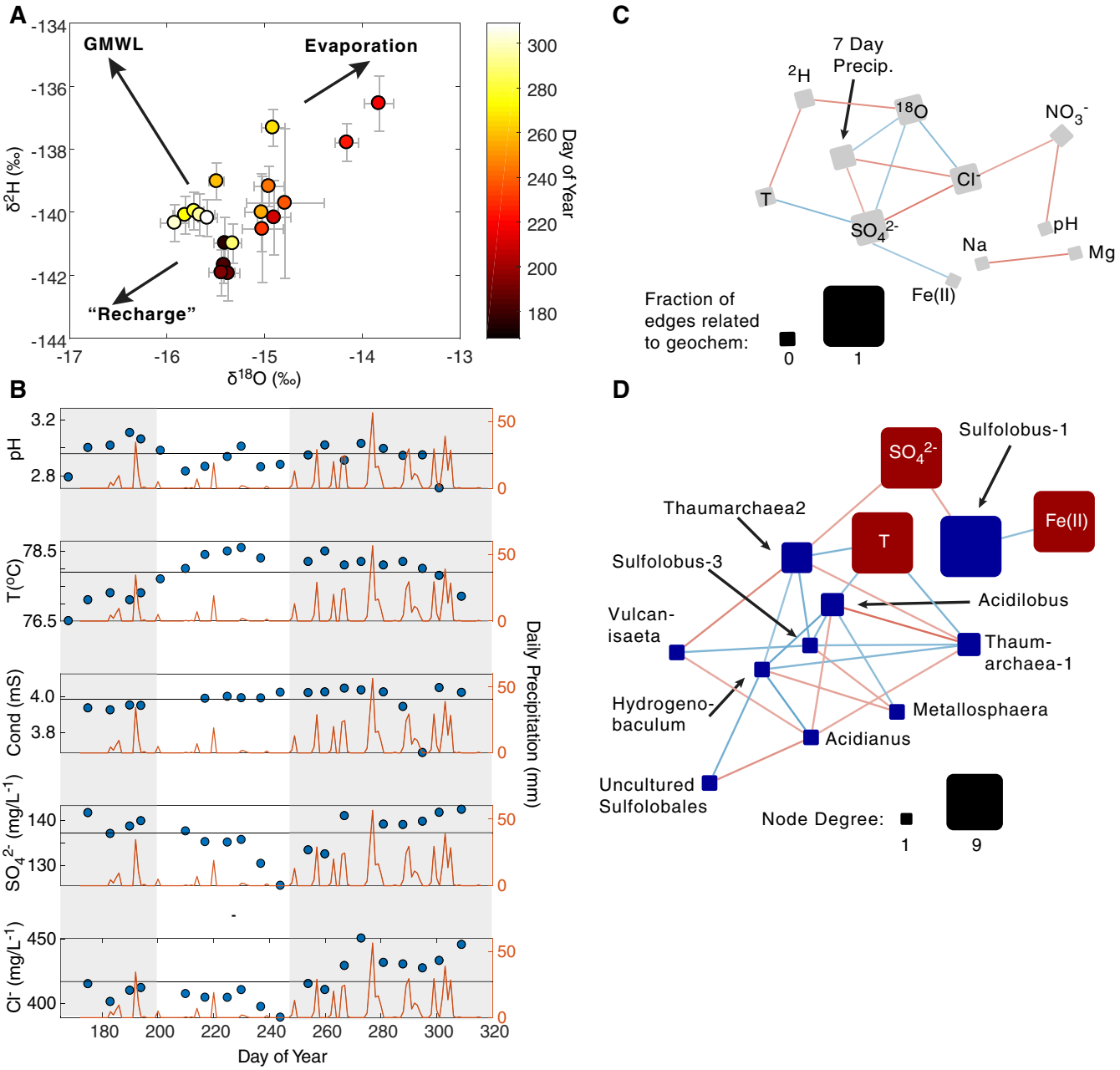

Fig. 6. Legend on next page.

heavier δ^2H and δ^{18}O values in the mid-summer samples were reversed in three mid-season samples taken between 12 August and 25 August (J.D. 225–238; Fig. 7A; Supplementary Table S1). The average δ^{18}O value for these three CP samples was -10.23 ± 0.25‰, in contrast to the average for the other mid-season CP samples at -8.88 ± 0.49‰. It is not clear what caused this shift in the δ^{18}O value of waters during this sampling interval.

The temperature in CP was considerably lower in the early and late summer/autumn than the near-boiling temperatures measured mid-season, with fluctuations up to 10°C (Fig. 7B). Variation in temperature was significantly and positively correlated with variation in conductivity (Fig. 7C; Pearson's $r = 0.59$, $p < 0.01$). Likewise, trends in SO_4^{2-} and Cl^- concentrations in CP waters were also positively correlated (Fig. 7C; Pearson's $r = 0.84$, $p < 0.0001$) and increased from early to mid-summer followed by a return in late summer to values close to those of the early summer waters (Supplementary Fig. S7). In contrast, pH slightly decreased from early to mid-summer and remained lower through late summer/autumn. These observations are interpreted to reflect dilution of the HO waters sourcing CP in early and later summer/autumn by input of meteoric water. Decreased dilution of these waters in the mid-summer, when local precipitation was minimal, could explain the increased Cl^- concentrations, SO_4^{2-} concentrations, temperature and conductivity during this time. This interpretation is generally supported by heavier water isotopes over this time interval, not considering the three anomalously lighter mid-summer isotope values that appeared after the only significant precipitation events of mid-summer. The trends in pH are not readily explainable, unless the hydrothermal-only (HO) type aquifer predominantly sourcing this spring is itself acidic (i.e. with a pH < 3), which would be consistent with a theorized acid-sulfate-chloride reservoir underlying the NGB (Truesdell *et al*., 1977, White *et al*., 1988, Fournier *et al*., 2002).

Like HFS communities, those of CP were dominated by the same uncultured Sulfolobales OTU with a much lower contribution from *Acidilobus* sp. and minor contributions from other populations (Fig. 3C). As with HFS waters, CP waters appeared to be responsive to dynamics in short-term precipitation. The effects of short-term precipitation may be primarily through dilution of the aquifer sourcing CP, as discussed above and evinced by negative correlations between 7-day precipitation and temperature and Cl^- concentrations in this spring (Fig. 7C). The relative abundance of the uncultured Sulfolobales OTU was negatively correlated with temperature in CP (Fig. 7D), while *Acidilobus* OTUs exhibited positive correlations with temperature and negative correlations with the uncultured Sulfolobales (Fig. 7D). Likewise, other OTUs were negatively correlated with the relative abundances of the uncultured Sulfolobales OTU, including those affiliated with *Vulcanisaeta* and *Hydrogenobaculum* (Fig. 7D). Consequently, it is possible that these patterns represent the outcomes of competitive interactions among these populations, where the uncultured Sulfolobales can outcompete other taxa for S compounds as electron donors (as inferred from genomic reconstructions) under (micro)oxic conditions. This includes *Vulcanisaeta* and *Acidilobus* that use S^0 as an electron acceptor under anoxic conditions (Itoh *et al*., 2002; Boyd *et al*., 2007) and *Hydrogenobaculum* that use S^0 as an electron donor under oxic conditions, but at lower temperatures than that of Sulfolobales (D'imperio *et al*., 2008; Boyd *et al*., 2009; Reysenbach *et al*., 2009).

Fig. 6. Seasonal variation in 'Dragon' Spring (DS) geochemical parameters and network analysis of associations among measured geochemical parameters and 16S rRNA gene operational taxonomic units (OTUs).

A. Water isotope values with each sample coloured according to the time scale next to the panel. Arrows are shown to indicate the general directions associated with water sources or processes (e.g. 'Recharge' representing the hypothesized recharge values for the YNP hydrothermal system discussed in Fig. 2; GMWL indicating the relative position of the Global Mean Water line; and Evaporation indicating the inferred direction of change upon hydrothermal boiling/evaporation.

B. Seasonal trends for geochemical parameters. The Julian calendar days corresponding to when measurements were made or when samples were collected and preserved for measurement are shown. Geochemical data are overlaid on daily rainfall shown in the orange traces. The early and late seasonal periods are shaded in grey boxes to help delineate seasonal periods, as defined in Fig. 1. The average value for a specified measurement for each is indicated by a black line.

C. Network depicting significant correlations ($p < 0.05$) among geochemical parameters for DS samples. Node sizing reflects fraction of edges related to geochemical parameters and is indicated by the scale to the bottom left of the network, with red edges indicating significant positive correlations and blue edges indicating significant negative correlations. Thus, larger-sized nodes represent geochemical parameters that exhibit more significant correlations to other geochemical parameters. Geochemical parameters without significant correlations to other parameters are not shown.

D. Network analyses of OTUs based on significant ($p < 0.05$) associations of their abundances with those of other OTUs and/or geochemical parameters. Node sizes are scaled to overall degree in the full network, as indicated in the bottom right of the figure, with edge colouring the same as in (C). Note that only geochemical parameters directly relevant to microbial metabolism are shown in this sub-network. The geochemical parameter nodes are all scaled to the same size, since the focus of the panel is to show the connectedness of OTUs to other OTUs and/or geochemical parameters only. Geochemical parameters that do not exhibit correlations to OTU abundances are not shown in these sub-networks. Geochemical parameter nodes are shown in red and OTU nodes are shown in blue. [Color figure can be viewed at wileyonlinelibrary.com]

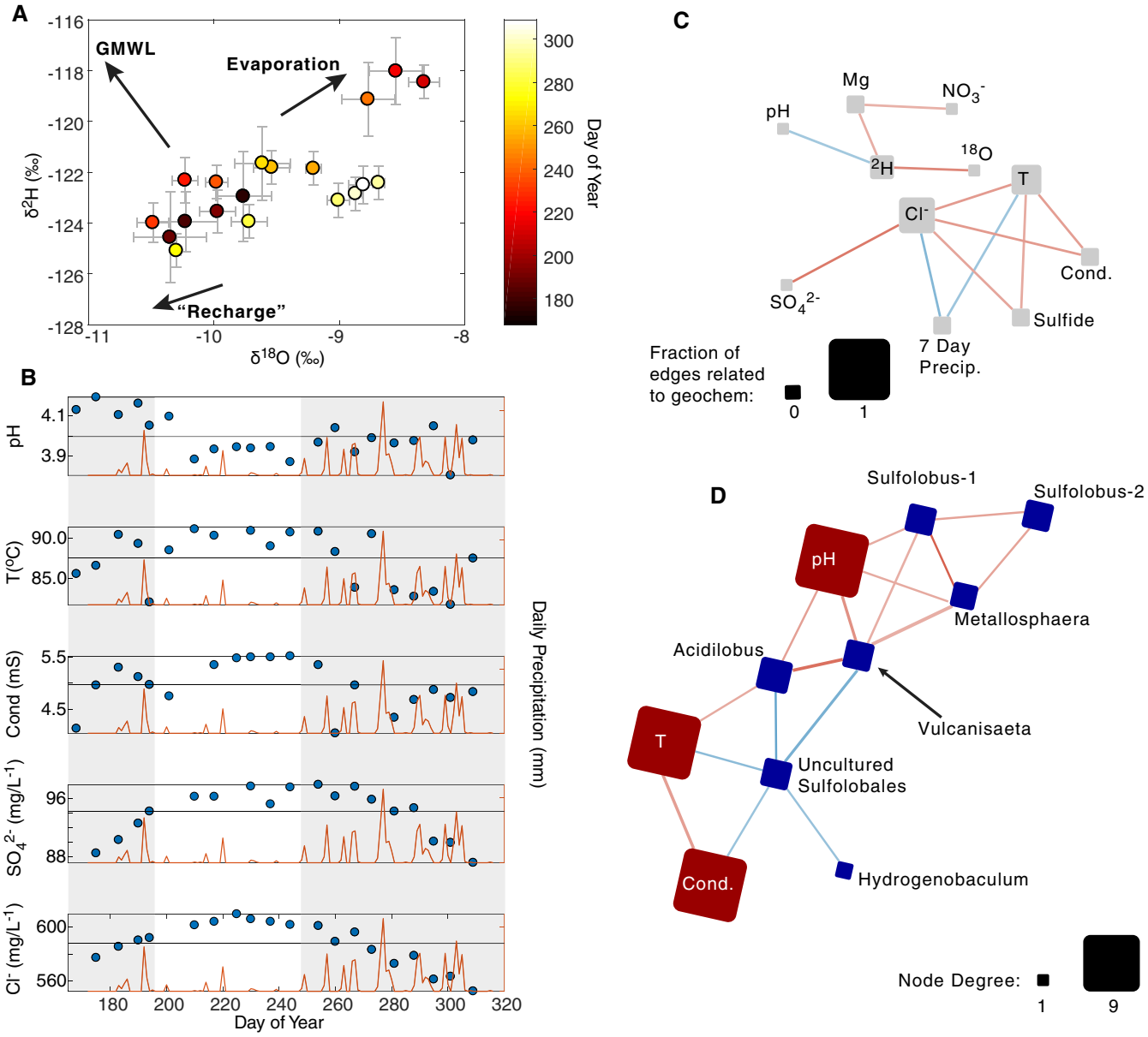

Fig. 7. Seasonal variation in Cinder Pool (CP) geochemical parameters and network analysis of associations among measured geochemical parameters and 16S rRNA gene operational taxonomic units (OTUs).
A. Water isotope values with each sample coloured according to the time scale next to the panel. Arrows are shown to indicate the general directions associated with water sources or processes (e.g. 'Recharge' representing the hypothesized recharge values for the YNP hydrothermal system discussed in Fig. 2; GMWL indicating the relative position of the Global Mean Water line; and Evaporation indicating the inferred direction of change upon hydrothermal boiling/evaporation.
B. Seasonal trends for geochemical parameters. The Julian calendar days corresponding to when measurements were made or when samples were collected and preserved for measurement are shown. Geochemical data are overlaid on daily rainfall shown in the orange traces. The early and late seasonal periods are shaded in grey boxes to help delineate seasonal periods, as defined in Fig. 1. The average value for a specified measurement for each is indicated by a black line.
C. Network depicting significant correlations ($p < 0.05$) among geochemical parameters for CP samples. Node sizing reflects fraction of edges related to geochemical parameters and is indicated by the scale to the bottom left of the network, with red edges indicating significant positive correlations and blue edges indicating significant negative correlations. Thus, larger-sized nodes represent geochemical parameters that exhibit more significant correlations to other geochemical parameters. Geochemical parameters without significant correlations to other parameters are not shown.
D. Network analyses of OTUs based on significant ($p < 0.05$) associations of their abundances with those of other OTUs and/or geochemical parameters. Node sizes are scaled to overall degree in the full network, as indicated in the bottom right of the figure, with edge colouring the same as in (C). Note that only geochemical parameters directly relevant to microbial metabolism are shown in this sub-network. The geochemical parameter nodes are all scaled to the same size, since the focus of the panel is to show the connectedness of OTUs to other OTUs and/or geochemical parameters only. Geochemical parameters that do not exhibit correlations to OTU abundances are not shown in these sub-networks. Geochemical parameter nodes are shown in red and OTU nodes are shown in blue. [Color figure can be viewed at wileyonlinelibrary.com]

Successional geochemical and microbial community dynamics in NS

The δ^2H and $\delta^{18}O$ values of NS generally trended lighter across the sampling period, potentially reflecting increased dilution of the aquifer sourcing the spring by meteoric water with time (Fig. 8A). This is potentially consistent with our visual observations that the OHSP ground became inundated with water due to rainfall near to the time that NS was first detected. These observations point to heavy precipitation in late summer/autumn as being at least partially responsible for the re-emergence of this spring after nearly 30 years of presumed dormancy, absent an alternative explanation for its emergence.

The pH of NS waters decreased after the spring first appeared and this was concomitant with an increase in temperature. Conductivity, SO_4^{2-} concentrations, and Cl^- concentrations were highly variable (Fig. 8B; Supplementary Fig. S7). Water isotope data suggest a trend towards increasing dilution of the aquifer sourcing this spring by meteoric water, which could explain the decrease in pH via enhanced aerobic sulfide or S^0 oxidation. However, these data are potentially inconsistent with increased temperature during this time, which would not necessarily be expected if the near-surface aquifer is being diluted with cold meteoric water (Fig. 8B). A possible reconciliation of these observations is that the spring also experienced increased input of high-temperature volcanic gas, which is supported by the higher dissolved sulfide concentrations in NS over time (Supplementary Fig. S12). Thus, we suggest that the water sourcing NS was progressively diluted by oxidized meteoric water and/or subjected to an increased input of high-temperature volcanic gas resulting in higher water temperatures, that together allowed for increased abiotic or biotic oxidation of S compounds leading to decreased pH (Fig. 8B). This interpretation is consistent with the appearance of this spring only after substantial rainfall had taken place and with visual observations of increasing S^0 deposition, an intermediate in the oxidation of sulfide (Nordstrom *et al*., 2005), in the spring outflow channel during the sampling period (Supplementary File S1). In addition to the increased development of S^0 deposition zones around the NS source and outflow channel with time, increasingly visible orange mineral depositions likely attributable to iron (hydr)oxides were observed immediately adjacent to the S^0 deposition zones (Supplementary File S1), suggesting the potential for biological iron oxidation as observed in other acidic springs in the OHSP (Macur *et al*., 2004).

The predominant OTU in NS immediately after the spring formed was related to an anaerobic S^0 reducing *Acidilobus* sp. (Supplementary Table S2), with minor contributions from the uncultured Sulfolobales phylotype discussed above (Fig. 3D). Shortly thereafter, the community shifted to being dominated by a *Hydrogenobaculum* sp. that then began to decline in relative abundance over the next month. During this period, increased abundances of *Metallosphaera*, a *Sulfolobus* sp. distinct from that discussed for HFS and CP, and Thaumarchaeota-related OTUs were observed. On 9 November, NS was sampled again and sequencing data indicated that the community shifted to near dominance by a *Metallosphaera* sp. and *Sulfolobus* spp. (Fig. 3D). These abrupt changes were consistent with considerable variation in predicted functional potential of NS communities over time, with sulfur reduction potential being prominent in the earliest samples, followed by S^0 oxidation (via primarily bacterial-type S^0 oxidation pathways) and SO_4^{2-}/SO_3^{2-} reduction metabolisms, and all followed by a final transition to dominance by archaeal-type S^0 oxidation (*Sulfolobus* or *Metallosphaera*) and inferred ferrous iron oxidation (*Metallosphaera*).

The dominance of the NS community by a *Hydrogenobaculum* OTU that is closely related to isolates capable of H_2S/S^0 oxidation after the spring formed is potentially consistent with S^0 deposition at NS beginning on 9 September that qualitatively appeared to increase in abundance with time (Supplementary File 1). The abrupt increase in SO_4^{2-} concentration (Fig. 8B) is coincident with *Hydrogenobaculum* dominance on 29 September (Fig. 3D), followed by subsequent decreased SO_4^{2-} concentrations (Fig. 8D) and decreased *Hydrogenobaculum* abundances (Fig. 3D). This could again point to the role of *Hydrogenobaculum* in mediating aerobic sulfur cycling in this spring. The S^0 oxidation activities of *Hydrogenobaculum* in NS are likely promoted by relatively lower water temperatures compared with the other springs, consistent with the significant negative correlation of temperature to SO_4^{2-} (Fig. 8C) and *Hydrogenobaculum* abundances (Fig. 3D), while *Hydrogenobaculum* abundances were positively correlated with SO_4^{2-} concentrations (Fig. 8D). *Hydrogenobaculum* isolates are known to optimally grow at ~55–65°C (Stohr *et al*., 2001; Donahoe-Christiansen *et al*., 2004; Dopson, 2016), which may ultimately bound their contribution to sulfur cycling in relatively lower temperature niches. Lastly, the concentrations of NO_3^- in NS were significantly associated with the abundances of the *Metallosphaera* OTU and those of one of the *Sulfolobus* sp. OTUs (Fig. 8D). NO_3^- concentrations were only related to OTU abundances in one other spring, HFS. Little is known about the source of NO_3^- within hot springs, although it is generally considered to be derived from the input of meteoric waters or the input of surface runoff (Bedinger *et al*., 1979), since there is little evidence for biological nitrification in acidic hot springs. Thus, the

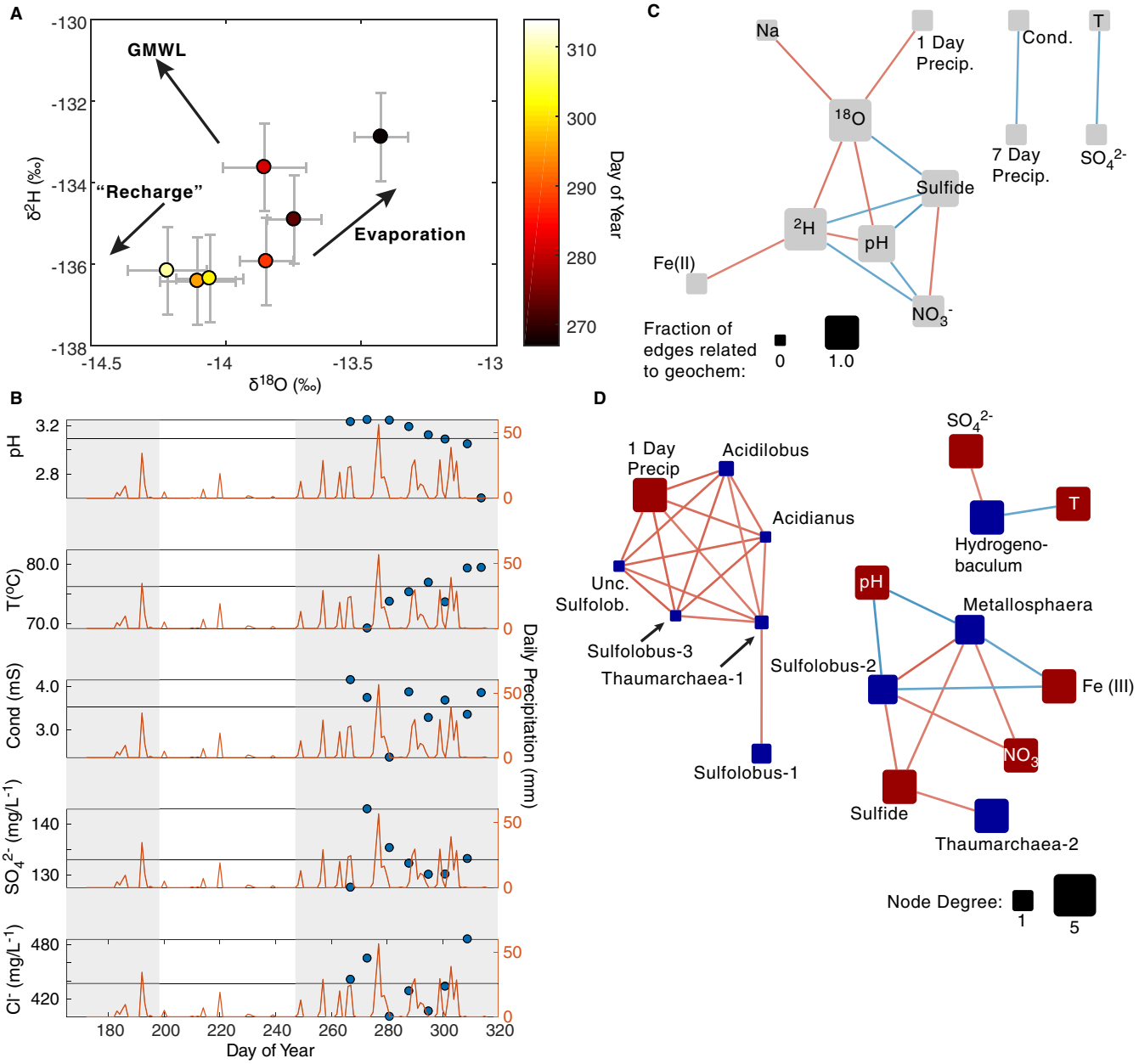

Fig. 8. Seasonal variation in 'New' Spring (NS) geochemical parameters and network analysis of associations among measured geochemical parameters and 16S rRNA gene operational taxonomic units (OTUs).
A. Water isotope values with each sample coloured according to the time scale next to the panel. Arrows are shown to indicate the general directions associated with water sources or processes (e.g. 'Recharge' representing the hypothesized recharge values for the YNP hydrothermal system discussed in Fig. 2; GMWL indicating the relative position of the Global Mean Water line; and Evaporation indicating the inferred direction of change upon hydrothermal boiling/evaporation.
B. Seasonal trends for geochemical parameters. The Julian calendar days corresponding to when measurements were made or when samples were collected and preserved for measurement are shown. Geochemical data are overlaid on daily rainfall shown in the orange traces. NS only appeared during the late seasonal period and thus, measurements are only shown following its emergence. The average value for a specified measurement for each is indicated by a black line.
C. Network depicting significant correlations ($p < 0.05$) among geochemical parameters for NS samples. Node sizing reflects fraction of edges related to geochemical parameters and is indicated by the scale to the bottom left of the network, with red edges indicating significant positive correlations and blue edges indicating significant negative correlations. Thus, larger-sized nodes represent geochemical parameters that exhibit more significant correlations to other geochemical parameters. Geochemical parameters without significant correlations to other parameters are not shown.
D. Network analyses of OTUs based on significant ($p < 0.05$) associations of their abundances with those of other OTUs and/or geochemical parameters. Node sizes are scaled to overall degree in the full network, as indicated in the bottom right of the figure, with edge colouring the same as in (C). Note that only geochemical parameters directly relevant to microbial metabolism are shown in this sub-network. The geochemical parameter nodes are all scaled to the same size, since the focus of the panel is to show the connectedness of OTUs to other OTUs and/or geochemical parameters only. Geochemical parameters that do not exhibit correlations to OTU abundances are not shown in these sub-networks. Geochemical parameter nodes are shown in red and OTU nodes are shown in blue. [Color figure can be viewed at wileyonlinelibrary.com]

correlations between OTU abundances in NS (and HFS) with NO_3^- concentrations likely reflect the strong association among geochemical parameters and microbial community compositions to seasonally variable inputs of meteoric waters to these springs.

Conclusions

Data presented here indicate that recent precipitation impacts the hydrologic properties of the near-surface aquifer(s) in the NGB of YNP and that this, in turn, differentially influences hot spring geochemistry and microbiology. The springs in this study exhibited varying responses to precipitation, with HFS exhibiting evidence of highly significant geochemical and microbiological changes in association with precipitation events, CP exhibiting intermediate to weak changes, and DS exhibiting minimal to no changes in response to precipitation. Perhaps most dramatically, NS emerged during the sampling period and this was at least partly attributed to heavy late summer/autumn precipitation, with evidence of geochemical and microbiological succession during the remainder of the sampling period. To our knowledge, this is the first coupled geochemical and microbiological investigation of a newly formed spring and therefore provides novel insight into the natural succession of hydrothermal microbial communities and their geochemical environment, both of which are influenced by the interplay between geology and hydrology. It should also be noted that the OTU definition used here (>97% nucleotide identity) may not sensitively capture more subtle changes in microbial taxonomic and functional variation that could accompany relatively subtle geochemical fluctuations. Thus, future studies should evaluate the potential intra-species or -strain differences associated with hot spring successional dynamics.

The observation that hot spring geochemistry and biodiversity are susceptible to changes in precipitation raises the intriguing possibility that these components of hot springs may be even more sensitive to sustained, long-term changes in precipitation or the extent and duration of snowpack. Warmer temperature regimes in the northern Rocky Mountains, including YNP, are expected due to changing climate regimes (Joyce *et al*., 2017). These changes can be expected to result in changes in the extent of precipitation and the longevity of snowpack that together may affect the magnitude and timing of recharge of deep and near-surface aquifers that source hot springs, with subsequent impacts on hot spring geochemistry and microbiology. It should be noted that the acidic springs analysed herein are likely more susceptible to changes in short-term recharge of aquifers due to the substantial input of meteoric waters to these spring types. For example, acidic springs exhibit mean water residence times estimated to be <200 years (Gardner *et al*., 2011) when compared to circumneutral or alkaline springs that are predominantly sourced by deeply sourced hydrothermal aquifers with much longer residence times, perhaps on the order of thousands of years (Pearson and Truesdell, 1978, Sturchio *et al*., 1987). Thus, acidic springs and acidophile biodiversity may be acutely and uniquely susceptible to changes in precipitation and meteoric recharge of aquifers that could accompany altered hydrologic cycles.

Although the effects of hydrologic forcing on the geochemistry and biodiversity of hot springs may be subtle, as observed for springs like DS and CP, they may also be significant, as evinced by the turnover of putative S^0-oxidizing populations in HFS across seasons and the emergence, establishment, and succession of NS and its community. The biodiversity of acidic springs such as in the NGB is relatively limited. However, weakly acidic springs are likely to be much more sensitive to near-term hydrologic forcing due to the stronger contribution of meteoric waters that source them. Several studies of moderately acidic springs reveal them to be biodiversity hotspots (Barns *et al*., 1994; Hugenholtz *et al*., 1998; Shock *et al*., 2005; Colman *et al*., 2019) and it is possible that hydrologic changes are likely to also alter, perhaps more significantly, their geochemical and microbiological composition. Thus, the data presented here provide new insights into the temporal dynamics of high-temperature hot spring biodiversity and warrant additional targeted studies to comprehensively understand the precise temporal scales at which microbial diversity responds to environmental fluctuations and whether these dynamics are restricted to specific types of springs or springs within specific geologic settings.

Experimental procedures

Sample collection

The four springs sampled in this study are in the OHSP of the Norris Geyser Basin (NGB) of Yellowstone National Park (YNP) (Supplementary Fig. 1). DS (44.731816 N, 110.710919 W; YNP Research Coordination Network thermal inventory ID: NHSP042), CP (44.732444 N, 110.709779 W; NHSP103), HF Spring (HFS; 44.733245 N, 110.709712 W; NHSP101) and a spring that manifested during sampling, NS (NS44.732611 N, −110.709750 W; not present within the RCN) are all within ∼500 m of one another (Supplementary Fig. 1). Planktonic communities were sampled from each of the four springs at near-weekly intervals between 23 June, 2016 and 4 November, 2016 using previously described methods (Colman *et al*., 2016), with one additional sample taken only for NS on 9 November, 2016. Briefly, 2 L of water (∼0.5 L from CP

due to suspended solid content) was collected aseptically from each spring at each sampling event (over the course of ~20–30 min) and filtered using 0.22 μm Sterivex® filters (EMD Millipore, Billerica, MA, USA) that were frozen in the field on dry ice and stored in a −80°C freezer in the laboratory. Water was also filtered with a 1.2 μm pre-filter followed by 0.8/0.2 μm Supor® filters (Pall, Port Washington, NY, USA) for use in geochemical analyses, using previously described methods (Colman *et al*., 2016) and in greater detail in the Supplementary Methods. All waters were sampled from the same point, nearest to the source that could be feasibly sampled and from the same depth to ensure appropriate comparison of samples across time.

Geochemical analyses

The pH, temperature and conductivity of hot spring waters were determined in the field, as previously described (Colman *et al*., 2016). Fe(II) and total sulfide were determined colorimetrically using a portable field spectrophotometer, as previously described (Lindsay *et al*., 2018). Triplicate sulfide and Fe(II) measurements were made and the averages are presented in Supplementary Table S1, except where otherwise noted. Major anions were determined via ion chromatography on a Dionex DX-600 system as previously described (Lindsay *et al*., 2018) (additional details in the Supplementary Methods), while stable hydrogen and oxygen isotope ratio (δ^2H and δ^{18}O) values of waters were determined via cavity ring-down spectroscopy, as previously described (Lindsay *et al*., 2018). Hourly rainfall measurements were retrieved from the UNAVCO NGB borehole B950 weather station (44.7128 N–110.6785 W; https://www.unavco.org/data/strain-seismic/seismic-data/seismic-data.html). The weather station is located ~3.3 km to the east of the springs on an outcrop of Lava Creek Tuff at an elevation of 2338 m that is roughly 57 m higher than the springs. Hourly rainfall measurements were summed for each day and these were subjected to calculation of a 7-day moving mean in precipitation (only considering the previous 7 days' values) with the 'movmean' function in the MATLAB computing environment. Additional geochemical data were compiled from previously published surveys of YNP springs (Ball *et al*., 2006; McCleskey *et al*., 2014) to contextualize the geochemistry of the springs sampled here.

Microbial community compositional analyses

Sterivex filters were removed from their plastic casings using a flame-sterilized coping saw and forceps, subjected to DNA extraction, PCR amplification, and DNA sequencing as previously described (Colman *et al*., 2016) and in additional detail in the Supplementary Methods. A total of 15 037 840 paired-end sequence reads were subjected to quality filtering as previously described (Kozich *et al*., 2013; Colman *et al*., 2016), removal of singleton sequences, and comparison against an acidic YNP hot spring metagenome-derived 16S rRNA gene database to identify potential 'contaminants', as described in additional detail in the Supplementary Methods. The final dataset comprised 54 samples and 6 881 160 non-singleton sequences that were sub-sampled to 22 488 sequence reads per sample. The subsampled dataset was used to evaluate among-community compositional differences based on the Bray–Curtis distance metric, as implemented in the 'vegdist' function of the vegan package (v.2.5-4) for the R computing environment (v.3.4.1; https://cran.r-project.org/web/packages/vegan/index.html). Samples were classified based on the time period in which they were sampled in (i.e. early, mid, and late seasons) and subjected to a permutational multivariate analysis of variance (PERMANOVA) test using the adonis2 function with vegan. The associations among abundant OTUs and geochemical parameters in each spring were evaluated with Pearson's correlational analyses and visualized via correlation networks (additional details in the Supplementary Methods).

To evaluate the functional potential of the spring communities and their inferred temporal variance, a genomic database was constructed to represent the 11 OTUs that contributed to >5% of any given community (Supplementary Table S2). A representative 16S rRNA gene OTU was chosen for each of these OTUs and compared to public genomic databases comprising hot spring isolate genomes and MAGs. Genomes (or MAGs) were then chosen when they matched representative OTUs at >98% nt identity and also comprised a complete or nearly complete genome. The Kyoto Encyclopedia of Genes and Genomes (KEGG) orthologue (KO) annotations for the genomes were then downloaded either from their host database (e.g. the Joint Genome Institute Integrated Microbial Genomes, JGI-IMG, server) or from the original publishing study. In addition, a subset of proteins that are poorly annotated within the KEGG database, but are integral components of dissimilatory sulfur metabolism pathways (Payne *et al*., 2019; Zeldes *et al*., 2019) were also searched against the encoded proteins using BLASTp searches with reference sequences (Payne *et al*., 2019, Zeldes *et al*., 2019) (Supplementary Table S3). The KO groups/BLAST homologues were then enumerated for each genome and multiplied by the relative abundance of the OTU for each sample to construct matrices for each sample that reflected the 'relative abundance' of inferred protein functions. Lastly, individual homologue annotations were summed for a given community sample to represent relative enrichment values and $\log_{10}$-transformed

to facilitate visualization. The overall differences in community functional profiles were also subject to statistical analyses using PERMANOVA to evaluate changes across springs or with seasonality, as described above for 16S rRNA gene community matrices.

Acknowledgements

This work was supported by a grant from the National Science Foundation to D.R.C. and E.S.B. (EAR-1820658). E.L.S., K.M.F. and R.V.D. acknowledge support from NASA Exobiology (NNX16AJ61G). M.B.S. was supported by a Fulbright US Scholar Award and the GNS Science GRN programme. A.H. and M.B.S. were supported by the Montana State University Undergraduate Scholars Program. Funding for 16S rRNA gene sequencing was provided by an American Geosciences Institute/Deep Carbon Observatory grant to D.R.C. We thank Christie Hendrix, Stacey Gunther and Annie Carlson at YNP for research permitting.

Data availability statement

The raw sequence reads generated from this study are available in the NCBI sequence read archive (SRA) under the Bioproject accession PRJNA661291.

References

Allen, E.T., and Day, A. (1935) *Hot Springs of the Yellowstone National Park*. Washington, DC: Carnegie Institute of Washington Publications.

Ball, J.W., McCleskey, R.B., Nordstrom, D.K., and Holloway, J.M. (2006) Water-chemistry data for selected springs, geysers, and streams in Yellowstone National Park, Wyoming. 1999–2000 U.S. Geol. Surv. Open File Rep., 02-382.

Barns, S.M., Fundyga, R.E., Jeffries, M.W., and Pace, N.R. (1994) Remarkable archaeal diversity detected in a Yellowstone National Park hot spring environment. *Proc Natl Acad Sci U S A* **91**: 1609–1613.

Bedinger, M.S., Pearson Jr., F.J., Reed, J.E., Sniegocki, R. T., and Stone, C.G. (1979) The waters of Hot Springs National Park, Arkansas - Their nature and origin.U.S.G. S. Open Report 1044-C.

Boyd, E.S., Jackson, R.A., Encarnacion, G., Zahn, J.A., Beard, T., Leavitt, W.D., *et al*. (2007) Isolation, characterization, and ecology of sulfur-respiring Crenarchaea inhabiting acid-sulfate-chloride-containing geothermal springs in yellowstone national park. *Appl Environ Microb* **73**: 6669–6677.

Boyd, E.S., Leavitt, W.D., and Geesey, G.G. (2009) CO_2 uptake and fixation by a thermoacidophilic microbial community attached to precipitated sulfur in a geothermal spring. *Appl Environ Microb* **75**: 4289–4296.

Brock, T.D., and Mosser, J.L. (1975) Rate of sulfuric acid production in Yellowstone National Park. *Geol Soc Am Bull* **86**: 194–198.

Colman, D.R., Feyhl-Buska, J., Robinson, K.J., Fecteau, K. M., Xu, H., Shock, E.L., and Boyd, E.S. (2016) Ecological differentiation in planktonic and sediment-associated chemotrophic microbial populations in Yellowstone hot springs. *FEMS Microbiol Ecol* **92**: 9.

Colman, D.R., Lindsay, M.R., and Boyd, E.S. (2019) Mixing of meteoric and geothermal fluids supports hyperdiverse chemosynthetic hydrothermal communities. *Nat Commun* **10**: 681.

Colman, D.R., Poudel, S., Hamilton, T.L., Havig, J.R., Selensky, M.J., Shock, E.L., and Boyd, E.S. (2018) Geobiological feedbacks and the evolution of thermoacidophiles. *ISME J* **12**: 225–236.

Colman, D.R., Poudel, S., Stamps, B.W., Boyd, E.S., and Spear, J.R. (2017) The deep, hot biosphere: twenty-five years of retrospection. *Proc Natl Acad Sci U S A* **114**: 6895–6903.

Craig, H., Boato, G., and White, D.E. (1956) Isotope geochemistry of thermal waters: National Academy of Sciences. *Nat Res Council Pub* **19**: 29–39.

Craig, H. (1961) Isotopic Variations in Meteoric Waters. Science. *AAAS* **133**(3465): 1702–1703.

D'imperio, S., Lehr, C.R., Oduro, H., Druschel, G., Kuhl, M., and McDermott, T.R. (2008) Relative importance of H_2 and H_2S as energy sources for primary production in geothermal springs. *Appl Environ Microb* **74**: 5802–5808.

Donahoe-Christiansen, J., D'Imperio, S., Jackson, C.R., Inskeep, W.P., and McDermott, T.R. (2004) Arsenite-oxidizing *Hydrogenobaculum* strain isolated from an acid-sulfate-chloride geothermal spring in Yellowstone National Park. *Appl Environ Microbiol* **70**: 1865–1868.

Dopson, M. (2016) Physiological and phylogenetic diversity of acidophilic bacteria. In *Acidophiles: Life in Extremely Acidic Environments*, Johnson, D.B., and Quatrini, R. (eds). Norfolk, United Kingdom: Caister Academic Press.

Fournier, R.O. (1989) Geochemistry and dynamics of the Yellowstone National Park Hydrothermal System. *Annu Rev Earth Pl Sc* **17**: 13–53.

Fournier, R.O., Weltman, U., Counce, D., White, L.D., and Janik, C.J. (2002) Results of weekly chemical and isotopic monitoring of selected springs in Norris Geyser Basin, Yellowstone National Park during June-September, 1995. U.S. Geol. Surv. Open File Rep., 02-344.

Gardner, W.P., Susong, D.D., Solomon, D.K., and Heasler, H.P. (2011) A multitracer approach for characterizing interactions between shallow groundwater and the hydrothermal system in the Norris Geyser Basin area, Yellowstone National Park. *Geochem Geophys Geosyst* **12**: 1–17.

Hamilton, T.L., Boyd, E.S., and Peters, J.W. (2011) Environmental constraints underpin the distribution and phylogenetic diversity of *nifH* in the Yellowstone geothermal complex. *Microb Ecol* **61**: 860–870.

Heasler, H.P., Jawrowski, C., and Foley, D. (2009) Geothermal systems and monitoring hydrothermal features. In *Geological Monitoring*, Young, R., and Norby, L. (eds). Boulder, Colorado: Geological Society of America, pp. 105–140.

Huber, H., and Prangishvaili, D. (2006) Sulfolobales. In *The Prokaryotes*, Vol. **3**, Dworkin, M., Falkow, S., Rosenberg, E., Schleifer, K.H., and Stackebrandt, E. (eds). New York: Springer.

Hugenholtz, P., Pitulle, C., Hershberger, K.L., and Pace, N. R. (1998) Novel division level bacterial diversity in a Yellowstone hot spring. *J Bacteriol* **180**: 366–376.

Hurwitz, S., and Lowenstern, J.B. (2014) Dynamics of the Yellowstone hydrothermal system. *Rev Geophys* **52**: 375–411.

Hutchinson, R.A. (1978) Geological Setting of Sylvan Spring Thermal Area. MS Thesis. Iowa State University.

Inskeep, W.P., Jay, Z.J., Herrgard, M.J., *et al*. (2013b) Phylogenetic and functional analysis of metagenome sequence from high-temperature archaeal habitats demonstrate linkages between metabolic potential and geochemistry. *Front Microbiol* **4**: 95.

Inskeep, W.P., Jay, Z.J., Tringe, S.G., Herrgård, M.J., Rusch, D.B., and YNP Metagenome project steering committee & working group members. (2013a) The YNP metagenome project: environmental parameters responsible for microbial distribution in the Yellowstone geothermal ecosystem. *Front Microbiol* **4**: 67.

Itoh, T., Suzuki, K., and Nakase, T. (2002) *Vulcanisaeta distributa* gen. nov., sp. nov., and *Vulcanisaeta souniana* sp. nov., novel hyperthermophilic, rod-shaped crenarchaeotes isolated from hot springs in Japan. *Int J Syst Evol Microbiol* **52**: 1097–1104.

Jackson, C.R., Langner, H.W., Donahoe-Christiansen, J., Inskeep, W.P., and McDermott, T.R. (2001) Molecular analysis of microbial community structure in an arsenite-oxidizing acidic thermal spring. *Environ Microbiol* **3**: 532–542.

Joyce, L.A., Talbert, M., Sharp, D., and Stevenson, J. (2017) Historical and projected climate in the northern Rockies. In *Climate Change and Rocky Mountain Ecosystems Advances in Global Change Reserach*, Vol. **63**, Halofsky, J.E., and Peterson, D.L. (eds). Switzerland: Springer International Publishing, pp. 17–23.

Kamyshny, A., Jr., Druschel, G., Mansaray, Z.F., and Farquhar, J. (2014) Multiple sulfur isotopes fractionations associated with abiotic sulfur transformations in Yellowstone National Park geothermal springs. *Geochem Trans* **15**: 7.

Kharaka, Y.K., Thordsden, J.J., and White, L.D. (2002) Isotope and chemical compositions of meteoric and thermal waters and snow from the greater Yellowstone National Park region. U.S. Geol. Surv. Open File Rep. 02-194.

Kozich, J.J., Westcott, S.L., Baxter, N.T., Highlander, S.K., and Schloss, P.D. (2013) Development of a dual-index sequencing strategy and curation pipeline for analyzing amplicon sequence data on the MiSeq Illumina sequencing platform. *Appl Environ Microbiol* **79**: 5112–5120.

Kozubal, M.A., Macur, R.E., Jay, Z.J., Beam, J.P., Malfatti, S.A., Tringe, S.G., *et al*. (2012) Microbial iron cycling in acidic geothermal springs of Yellowstone National Park: integrating molecular surveys, geochemical processes, and isolation of novel Fe-active microorganisms. *Front Microbiol* **3**: 109.

Langner, H.W., Jackson, C.R., Mcdermott, T.R., and Inskeep, W.P. (2001) Rapid oxidation of arsenite in a hot spring ecosystem, Yellowstone National Park. *Environ Sci Technol* **35**: 3302–3309.

Lindsay, M.R., Amenabar, M.J., Fecteau, K.M., Debes, R.V., Martins, M.C.F., Fristad, K.E., *et al*. (2018) Subsurface processes influence oxidant availability and chemoautotrophic hydrogen metabolism in Yellowstone hot springs. *Geobiology* **16**: 674–692.

Lowenstern, J.B., Bergfeld, D., Evans, W.C., and Hurwitz, S. (2012) Generation and evolution of hydrothermal fluids at Yellowstone: insights from the Heart Lake Geyser Basin. *Geochem Geophys Geosyst* **13**: 1–20.

Macur, R.E., Langner, H.W., Kocar, B.D., and Inskeep, W.P. (2004) Linking geochemical processes with microbial community analysis: successional dynamics in an arsenc-rich, acid-sulphate-chloride geothermal spring. *Geobiology* **2**: 163–177.

Marler, G.D., and White, D.E. (1977) Evolution of seismic geyser, Yellowstone National Park. *Earthquake Inf Bull (USGS)* **9**: 21–25.

McCleskey, R.B., Chiu, R.B., Nordstrom, D.K., Campbell, K. M., Roth, D.A., Ball, J.W., and Plowman, T.I. (2014) Water-chemistry data for selected springs, geysers, and streams in Yellowstone National Park, Wyoming, beginning 2009. U.S. Geological Survey Open-File Report.

Nordstrom, D.K., McCleskey, R.B., and Ball, J.W. (2009) Sulfur geochemistry of hydrothermal waters in Yellowstone National Park: IV acid-sulfate waters. *Appl Geochem* **24**: 191–207.

Nordstrom, K.D., Ball, J.W., and McCleskey, R.B. (2005) Ground water to surface water: chemistry of thermal outflows in Yellowstone National Park. In *Geothermal Biology and Geochemistry in Yellowstone National Park*, Inskeep, W.P., and McDermott, T.R. (eds). Bozeman, MT: Montana State University, pp. 73–94.

Payne, D., Dunham, E.C., Mohr, E., Miller, I., Arnold, A., Erickson, R., *et al*. (2019) Geologic legacy spanning >90 years explains unique Yellowstone hot spring geochemistry and biodiversity. *Environ Microbiol* **21**: 4180–4195.

Pearson, F.J., and Truesdell, A.H. (1978) Tritium in the waters of Yellowstone National Park. In Short Papers of the Fourth International Conference, Geochronology, Cosmochronology, Isotope Geology, Zartman, R.E. (ed). Washington D.C: US Geological Survey, pp. 327–329.

Podar, M., Makarova, K.S., Graham, D.E., Wolf, Y.I., Koonin, E.V., and Reysenbach, A.L. (2013) Insights into archaeal evolution and symbiosis from the genomes of a nanoarchaeon and its inferred crenarchaeal host from Obsidian Pool, Yellowstone National Park. *Biol Direct* **8**: 9.

Reysenbach, A.L., Hamamura, N., Podar, M., Griffiths, E., Ferreira, S., Hochstein, R., *et al*. (2009) Complete and draft genome sequences of six members of the Aquificales. *J Bacteriol* **191**: 1992–1993.

Romano, C., D'Imperio, S., Woyke, T., Mavromatis, K., Lasken, R., Shock, E.L., and McDermott, T.R. (2013) Comparative genomic analysis of phylogenetically closely related *Hydrogenobaculum* sp. isolates from Yellowstone National Park. *Appl Environ Microbiol* **79**: 2932–2943.

Rye, R.O. (1993) The evolution of magmatic fluids in the epithermal environment; the stable isotope perspective. *Econ Geol* **88**: 733–752.

Rye, R.O., and Truesdell, A.H. (2007) The question of recharge to the deep thermal reservoir underlying the geysers and hot springs of Yellowstone National Park in

integrated geoscience studies in the Greater Yellowstone Area: volcanic, hydrothermal, and tectonic processes in the Yellowstone Geoecosystem, edited by L.A. Morgan, U.S. *Geol Surv Prof Pap* **1717**: 205–234.

Shock, E.L., Holland, M., Meyer-Dombard, D., Amend, J.P., Osburn, G.R., and Fischer, T.P. (2010) Quantifying inorganic sources of geochemical energy in hydrothermal ecosystems, Yellowstone National Park, USA. *Geochim Cosmochim Acta* **74**: 4005–4043.

Shock, E.L., Holland, M., Meyer-Dombard, D.R., and Amend, J.P. (2005) Geochemical sources of energy for microbial metabolism in hydrothermal ecosystems: Obsidian Pool, Yellowstone National Park. In *Geothermal Biology and Geochemistry in Yellowstone National Park*, Inskeep, W.P., and McDermott, T.R. (eds). Bozeman, MT: Montana State University, pp. 95–110.

Simon, G., Walther, J., Zabeti, N., Combet-Blanc, Y., Auria, R., van der Oost, J., and Casalot, L. (2009) Effect of O_2 concentrations on *Sulfolobus solfataricus* P2. *FEMS Microbiol Lett* **299**: 255–260.

Spear, J.R., Walker, J.J., McCollom, T.M., and Pace, N.R. (2005) Hydrogen and bioenergetics in the Yellowstone geothermal ecosystem. *Proc Natl Acad Sci U S A* **102**: 2555–2560.

Stohr, R., Waberski, A., Volker, H., Tindall, B.J., and Thomm, M. (2001) *Hydrogenothermus marinus* gen. nov., sp. nov., a novel thermophilic hydrogen-oxidizing bacterium, recognition of *Calderobacterium hydrogenophilum* as a member of the genus *Hydrogenobacter* and proposal of the reclassification of *Hydrogenobacter acidophilus* as *Hydrogenobaculum acidophilum* gen. nov., comb. nov., in the phylum '*Hydrogenobacter*/*Aquifex*'. *Int J Syst Evol Microbiol* **51**: 1853–1862.

Sturchio, N.C., Binz, C.M., and Lewis, C.H., III. (1987) Thorium-uranium disequilibirum in a geothermal discharge zone at Yellowstone. *Geochim Cosmochim Acta* **51**: 2025–2034.

Takacs-Vesbach, C., Inskeep, W.P., Jay, Z.J., *et al*. (2013) Metagenome sequence analysis of filamentous microbial communities obtained from geochemically distinct geothermal channels reveals specialization of three Aquificales lineages. *Front Microbiol* **4**: 84.

Truesdell, A.H., Nathenson, M., and Rye, R.O. (1977) Effects of subsurface boiling and dilution on isotopic compositions of Yellowstone thermal waters. *J Geophys Res* **82**: 3694–3704.

Urschel, M.R., Kubo, M.D., Hoehler, T.M., Peters, J.W., and Boyd, E.S. (2015) Carbon source preference in chemosynthetic hot spring communities. *Appl Environ Microb* **81**: 3834–3847.

Wang, S., Dong, H., Hou, W., Jiang, H., Huang, Q., Briggs, B.R., and Huang, L. (2014) Greater temporal changes of sediment microbial community than its waterborne counterpart in Tengchong hot springs, Yunnan Province, China. *Sci Rep* **4**: 7479.

Ward, L., Taylor, M.W., Power, J.F., Scott, B.J., McDonald, I. R., and Stott, M.B. (2017) Microbial community dynamics in Inferno Crater Lake, a thermally fluctuating geothermal spring. *ISME J* **11**: 1158–1167.

White, D.E., Keith, T.E.C., and Hutchinson, R.A. (1988) The geology and remarkable thermal activity of Norris Geyser Basin, Yellowstone National Park, Wyoming. U.S. Geol. Survey Prof. Paper 1456.

Xu, Y., Schoonen, M.A.A., Nordstrom, D.K., Cunningham, K. M., and Ball, J.W. (2000) Sulfur geochemistry of hydrothermal waters in Yellowstone National Park, Wyoming, USA II formation and decomposition of thiosulfate and polythionate in cinder Pool. *J Volcanol Geoth Res* **97**: 407–423.

Zeldes, B.M., Loder, A.J., Counts, J.A., Haque, M., Widney, K. A., Keller, L.M., *et al*. (2019) Determinants of sulphur chemolithoautotrophy in the extremely thermoacidophilic Sulfolobales. *Environ Microbiol* **21**: 3696–3710.

Zhang, J.-Z., and Millero, F.J. (1993) The products from the oxidation of H_2S in seawater. *Geochim Cosmochim Acta* **57**: 1705–1718.

Supporting Information

Additional Supporting Information may be found in the online version of this article at the publisher's web-site:

Appendix S1. Supplementary Information.

Supplementary Table S1. Geochemical data for samples taken during this study. 'n.d.' refers to not determined for that sample.

Supplementary Table S2. Additional information for the predominant operational taxonomic units (OTUs) identified in this study. Only OTUs with >5.0% relative abundance in any sample are shown. Taxonomic information is given for each, along with a representative 16S rRNA gene sequence, and information about the nearest characterized isolate or genome to the representative 16S rRNA gene sequences.

Supplementary Table S3. Description of genes used to infer functional profiles of populations within communities. The gene abbreviations correspond to those shown in Fig. 4. Catalytic activity is determined based on the provided reference for each gene or set of genes. In addition, the identification of each gene is indicated as either the presence of a KEGG KO ortholog within reference genomes, or via a BLAST search of the indicated protein against the encoded proteins of the reference genome.

Supplementary File S1. Images of 'New' Spring taken from the first day of observation through the sampling period of this study in addition to images from beyond the present study period.